2018

# MODELING THE MORPHOLOGICAL EVOLUTION OF STABILIZED DUNE SYSTEM DURING EXTREME STORM EVENTS

Naser Yusuf AlNaser
*University of Rhode Island*, nalnaser.99@gmail.com

# MODELING THE MORPHOLOGICAL EVOLUTION OF STABILIZED DUNE SYSTEM DURING EXTREME STORM EVENTS

BY

NASER ALNASER

A THESIS SUBMITTED IN PARTIAL FULFILLMENT OF THE REQUIREMENTS FOR THE DEGREE OF

MASTER OF SCIENCE

IN

OCEAN ENGINEERING

UNIVERSITY OF RHODE ISLAND

2018

MASTER OF SCIENCE THESIS

OF

NASER ALNASER

APPROVED:

Thesis Committee:

Major Professor Annette Grilli

Stephan Grilli

Aaron Bradshaw

Nasser H. Zawia
DEAN OF THE GRADUATE SCHOOL

UNIVERSITY OF RHODE ISLAND
2018

## ABSTRACT

The key role of beach dunes in protecting coastal developments from damages caused by seasonal storm and hurricanes (e.g. Hurricane Sandy 2012), prompted series of studies devoted to assess their stability during these conditions. A 2-D numerical study for a "100-year storm" event (1% probability of annual exceedance) in Rhode Island indicate extreme dune erosion can occur when these structural barriers become submerged during coastal flooding events, making them ephemeral solutions only (Schambach et al., 2018). In contrast, areas with dense vegetation experienced less morphological changes due to reduced wave energy. Model predictions however remain uncertain due to the lack of comparative studies with field data. The study provides a performance evaluation assessment of four modeling scenarios used to assess the stability of a vegetated dune system in barrier beaches during storm events. These are combination of two wave models (phase averaging vs. phase resolving) with two approaches to modeling the affect of vegetation on sediment transport (bed friction formulations vs. wave damping formulations). Best estimates of the post dune profiles were obtained when using the phase averaged wave model with vegetation described by bed friction coefficients. This scenario was able to predict accurate changes of the along shore crest height elevations, making it a good assessment tool for determining the vulnerability of coastal communities in Rhode Island.

In a second chapter, we address the potential use of Geotextile Sand-filled Containers (GSCs) to reinforce and stabilize a dune system during storm events. A new classification of the damage states associated with these "soft-structures" used for coastal protection are identified and described. Modeling approaches to identify each damage

level during a storm were validated using post survey measurements taken from a storm which caused damage to a new project site where reinforced dune system with GSCs was constructed. Two hydraulic stability formulas for GSCs were used to determine the critical conditions for the instability of the GSC structure. Results indicate lower confidence when using Hudson's (1956) based stability equations when compared with Recio and Oumeraci (2008) semi-empirical formulations. Overall good prediction of the damage levels was obtained when compared with measurements, suggesting a potential tool for predicting the stability of the structure.

## ACKNOWLEDGMENTS

Thanks goes to almighty God for giving me the opportunity, strength and knowledge to complete this study. My deepest gratitude and thanks also goes to my advisor Prof. Annette Grilli, who guided me throughout this research journey. Her dedication and mindset to this field inspired me toward a successful contribution. I shall always remain in debt to her insightful feedback and constant suggestions that resonates through this report. In addition, I wish to thank all the Professors who taught me during this program, and equipped me with the fundamental knowledge and skills to survive and complete this mission. Special thanks to Prof. Stephan Grilli, in which his courses in wave mechanics and surf-zone hydrodynamics reflected the most on me, and are echoed through this report. I also will never forget Prof. Christopher Baxter directives, which lead me to successfully meet my learning objectives. I further like to thank my colleague Brian Maggi, for sharing his doctoral research data, which were used in the second part of this study.

This research study of course would not have been possible without the support and funding of the US Department of State, Bureau of Education and Cultural Affairs through my Fulbright Scholarship. I also dedicate this work to the Ministry of Works, Municipalities Affairs and Urban Planning of the Kingdom of Bahrain, who encouraged me and further supported me to undertake this quest.

Last but not least, I am thankful to all my friends who made this journey adventurous and memorable, and to my family and more importantly my Parents for their enduring love and support.

## PREFACE

This thesis report concludes the Master of Science program in Ocean Engineering at the University of Rhode Island. It is presented in a manuscript format, and includes two chapters each talks about a different type of stabilized dune system. Chapter 1 discusses the applicability and limitation of certain approaches to model the effect of vegetation on sediment transport. Although the study focuses on vegetated dune systems in barrier beaches during extreme events, the approaches and conclusions of this study may also be suitable when considering the use of vegetation for general applications of coastal protections. The study was provoked by the tremendous effort taken by US federal agencies such as the National Oceanographic and Atmospheric Agency (NOAA), US Army Corps of Engineers (USACE), and the US Geological Survey (USGS) to provide qualitative large scale set of data on those areas affected by Hurricane Sandy 2012, as part of a national assessment of coastal change hazards.

Chapter 2 introduces a new level of classification for identifying the damage states associated with reinforced dunes with Geotextile Sand-filled Containers (GSCs). This soft "natural-based" solution for coastal protection was recently introduced in the United States, when the USACE funded the first project of its type in Montauk, NY. The potential use of GSCs in Rhode Island, have been considered, however validation of design codes and stability formulas for GSCs are required. The outcomes of this study will be used to plan and design a larger research study aimed to develop a fragility curve to predict the performance of these structures. Special thanks to USACE for disclosing essential project information and As-built measurements, and to Brian Maggi for sharing valuable data from his doctoral research and his assistance.

## TABLE OF CONTENTS

## LIST OF TABLES

## LIST OF FIGURES

# CHAPTER 1

## "Modeling the Effect of Vegetation On Dune Erosion During Extreme Storm Events"

by

Naser AlNaser[1]; Annette R. Grilli[2]; Stephan T. Grilli[3]

Prepared for submission to the Journal of Coastal Engineering

[1] MSc Student, Department of Ocean Engineering, University of Rhode Island, Narragansett, RI 02882. Email: nalnaser.99@gmail.com

[2] Associate Research Professor, Department of Ocean Engineering, University of Rhode Island, Narragansett, RI 02882. Email: annette_grilli@uri.edu

[3] Distinguished Professor and Chair, Department of Ocean Engineering, University of Rhode Island, Narragansett, RI 02882. Email: grilli@uri.edu

**Abstract**

Sea level rise and storm intensification lead to re-evaluate inundation assessments along the North Atlantic US shoreline. A particular effort is devoted to assess the coastal community risk to the “100-year storm“ event (1% probability of annual exceedance) in Rhode Island (RI), US, using a chain of state of the art storm surge, wave propagation, and coastal erosion 2-D models. As part of this effort, a recent study indicated that RI beach barriers covered with dense vegetation would experience less erosion and morphological changes than similar beach barriers barely vegetated, as expected from theoretical considerations and past studies (Schambach et al., 2018) The present study is cast in this context and provides a comparative analysis of selected hydro-morphodynamic approaches for predicting dune erosion and morphological changes of the dune system, in dissipative beaches and barrier islands, for various storm regimes as described by Sallenger (2000) using the 2-D model XBeach. In particular, we investigate the applicability, performance and limitations of the selected hydro-morphodynamic models regarding their ability to assess the vegetation’s effect on sediment transport during extreme storm events. We compare results of simulation for an historical storm (Sandy) using either a vegetation module based on Mendez and Losada’s formulation (2004), or a friction parameterization based on a Manning formulation. In addition, the sensitivity to the selected wave model, the Non-hydrostatic (Smit et al., 2010) and Surfbeat (Roelvink et al., 2009) models are investigated. Various performance capabilities and limitations are observed when each model was assessed during collision, overwash and inundation regime. Unresolved depth profile in XBeach lead to significant reduction in the depth averaged velocities and resulted in underestimation of the sediment transport

rate when using the vegetation module in overwash and inundation regime. Less energy dissipation occurred when using the bed friction parameterization approach and therefore better predictions of the morphological shape of the dune profile. Comparison between the two wave models indicated incompatibility when using the Van Thiel – Van Rijin 2009 sediment transport formulation with the Non-hydrostatic approach to estimate dune erosion rates in the overwash and inundation regime due to the dominancy of the short waves orbital velocities. Reasonable predictions of the crest elevations and morphological profile of the dune were obtained when using the Surbeat wave model for all regimes.

***Keywords**:* Beach barrier erosion, dune, XBeach, Surfbeat, Non-hydrostatic, vegetation

## 1. Introduction

Extreme stages of dune erosion have been common occurrences along the US North Atlantic coast exposing coastal communities to higher inundation risk than expected based on historical storms (e.g. Woodruff et al., 2013, 2006, Grilli et al., 2017a, 2017b). The anticipated increase frequency of extreme events due to climate change has incited coastal management agencies to take protective actions. Planting vegetation along dunes crest combined with protective measures restricting their usage is a traditional approach to stabilize dunes (e.g. Woodhouse et al. 1978; Knutson, 1977).

The vegetation indeed helps to maintain the dune. From an aeolian perspective, dunes increase roughness length (Charnock, 1955), increasing the loss of energy by friction and turbulence, resulting in a lower flow velocity, ultimately trapping the sand into the dune system. When the vegetation is submerged, similar hydrodynamics processes to the aerodynamics one affect the flow promoting local sedimentation. In

addition, trapped-sediments are protected from re-suspension due to the local deficit of energy in the flow, reinforcing the protective effect of the vegetation on the dune system (e.g. Gacia and Duarte, 2001; Manca et al., 2012).

The functional role of dune vegetation as a management tool to preserve the dune morphology and protect inland area from inundation has been abundantly documented, beginning with Cowles's ecological lesson (1899) relating dune morphology and "plant society. The idea of using natural and nature-based features (NNBF) between ocean and land such as dunes in particular acting as buffers to protect coastal communities however became recently increasingly popular in both the scientific and the coastal management community (e.g. Smith et al., 2016) leading to collaborative works between both stake holders (e.g., BEACH SAMP, RI). Some authors have attempted to assess the value of specific coastal ecosystems such as vegetated dunes, salt marshes and mangrove habitats in an Ecosystem-Based Management (EBM) approach (Aburto et al., 2012). Barbier et al. (2008) demonstrate an increase value in "coastal protection service", proportional to the vegetated habitat area.

In parallel, a need to provide numerical simulations for extreme storm scenarios with adequate accuracy to address the coastal communities risk, has emerged. Although modeling storm surge and wave propagation can be done with relative accuracy, modeling dune erosion accurately is more complex.

In this work we investigate the adequacy of four selected hydro-morphodynamic approaches for predicting dune erosion and morphological changes of the dune system in dissipative beaches and barrier islands, for various storm regimes as described by Sallenger (2000) using the 2-D model XBeach (Roelvink et al., 2009, 2010, 2018). In

particular, we investigate the applicability, performance and limitations of the selected hydro-morphodynamic models regarding their ability to assess the vegetation's effect on sediment transport during extreme storm events. We compare results of simulation for the historical storm Sandy using either a vegetation module based on Mendez and Losada's formulation (2004), or a friction parameterization based on a Manning formulation. In addition, the sensitivity to the selected wave model, the Non-hydrostatic (Smit et al., 2010, 2013, 2014) and Surf-beat (Roelvink et al., 2009, 2018) models, is investigated. The test site is located in an undeveloped vegetated barrier island beach close to Sandy's landfall location in New Jersey. Pre and Post survey LiDAR measurements of the bed level change were conducted by the US Army Corps of Engineers (USACE), and was used to validate and compare results. Further description of the land cover type was obtained from US Geological Survey (USGS).

A background summary is provided in Section 2. The methodology is presented in Section 3 with a presentation of the selected site and of the simulated scenarios, including a brief overview of the XBeach model. Data and model set up are presented in Section 4. Results are provided in Section 5. Discussion and conclusion are presented in Section 6 and 7 respectively.

## 2. Background

### *2.1 Key Conceptual Wok*

The use of vegetation to damp wave energy has been investigated for many decades theoretically and empirically. Price et al. (1969) proposed the deployment of artificial seaweeds in the surf-zone to limit coastal erosion in England, based on theoretical development as well as tank experiments. Dalrymple et al. (1984) modified Radder's

wave propagation parabolic model (1979) to include a term, which allows for the dissipation of wave energy associated to wave propagation across vegetation (Booij, 1981). The theory was restricted to damping induced by vegetation for non-breaking regular waves and horizontal bottom. Mendez and Losada (2004) expanded Dalrymple et al.'s (1984) theory to take into account the bottom variations, the randomness of the waves and the dissipation due to breaking in the surf zone. Although various formulations of the dissipation terms have been proposed, the standard formulation is based on a hypothetical array of rigid cylinders, to mimic stems, creating an additional drag force on the flow. Typically the plant-induced force acting on the fluid is expressed in terms of a Morison-type equation (Morison et al., 1950) neglecting swaying motion and inertia forces, lumping the uncertainty on the flexibility of and the relative configuration of the stems in an empirical drag coefficient. Consequently, the drag coefficient must be calibrated for specific vegetation stem types and patterns in either field studies or laboratory experiment. In later studies, this formulation has been modified to include the plant motion, coupling flow and vegetation motions (e.g. Stratigaki et al., 2011; Mendez et al., 1999; Mazda et al., 2013).

*2.2 Field and Laboratory Work*

Although many field and laboratory studies have focused on seagrass species present in the surf zone such as *Laminaria hyperborean* (e.g., in laboratory, Kobayashi et al., 1993; Dubi and Tørum, 1995; Løvås and Tørum, 2001; or in field, Anderson et al., 1996), *Zostera noltii* (in field, Paul and Amos, 2011) or *Posidonia Oceanica* (e.g. in laboratory, Sánchez-González et al., 2011; Stratigaki et al. 2011; Manca et al., 2012; Koftis et al., 2013), many authors have specifically addressed the sub-aerial vegetation submerged in

extreme storm surge conditions, often in field studies, such as trees in mangrove environment as *Kandelia candel*, (e.g. Mazda et al., 1997; Quartel et al., 2007) or *Sonneratia sp.*, *Avicennia marina* (Mazda et al., 2006; Vo-Luong and Massel, 2008; Hortsman et al., 2014), cordgrass in intertidal salt-marsh environment, as *Spartina Alterniflora* (e.g. Knutson et al., 1982; Cooper, 2005; Ysebaert et al., 2011; Jadhav et al., 2013) or mixed-salt marsh species (e.g., Moller et al., 1999, 2002, 2006; Cooper, 2005). In laboratory, most studies have focused salt marsh vegetation such as *Spartina Alterniflora* (e.g. Suzuki et al., 2012; Augustin et al., 2009; Anderson and Smith, 2014). Relatively few studies have focused on trees, usually in Mangrove environment (Massel et al., 1999; Irtem et al., 2009; Alongi, 2009). More complex theoretical formulations have been developed for trees trunk, acting at a larger scale than seagrass (Mei et al., 2011).

*2.3 Implementation of Vegetation Modules in Numerical Modules*

Semi-empirical formulations of energy dissipation associated with vegetation cover based on Mendez and Losada (2004) have been implemented into hydrodynamics models such as SWAN (Suzuki et al., 2012), STWAVE (Smith et al., 2016), NHWAVE (Ma et al., 2013) and into the hydro-morphodynamic model XBeach. This formulation provides an alternative method to assess the energy dissipation associated with vegetation to the standard friction approach in which the energy is dissipated through a friction coefficient, such as a Manning coefficient, reflecting the bed roughness associate to the specific land cover (Arcement and Schneider, 1989).

This later standard parametric method, using a spatially variable Manning coefficient with value associated to the specific land-cover, has been applied and discussed in many

applications using several hydrodynamics models (e.g, in STWAVE, Wamsley et al., 2009, 2010), and more recently using the hydro-morphodynamic model XBeach (Nederhoff, 2014; De Vet et al., 2015; Schambach et al., 2018). However, while the use of the Manning coefficient has been extensively validated for river discharges and channel flows (Vargas-Luna et al., 2015; Ishikawa et al., 2003; Jordanova and James, 2003; Thompson et al., 2004; Kothyari et al., 2009), validations in coastal applications with flow and currents induced by waves are still currently limited (e.g. Gacia and Duarte 2001; Terrados and Duarte, 2000).

Schambach et al. (2018) used a spatially variable Manning Coefficient as a function of the land cover for their 2-D model XBeach wave and erosion simulations across to simulate the erosion of the Charlestown barrier beach system along the southern shore of Rhode Island, U.S, for a conceptual 100-year storm. The author showed a significant spatial variability in dune erosion, and landward inundation as a function of the vegetation coverage of the dune. In that study the vegetation was parameterized using a spatially variable Manning coefficient as a function of the land cover.

**3. Methodology**

In this work we investigate the adequacy of both (1) the friction parameterization based on a spatially variable Manning coefficient as a function of the vegetation cover, and (2) the vegetation module based on Mendez and Losada's formulation (2004) as implemented in XBeach to simulate dune erosion for three of Sallenger's erosion stages, collision, overwash and inundation using the 2-D model XBeach at our test site, a barrier beach in U.S. North East Atlantic Coast. Results of simulations are compared with observations after Super-storm Sandy hit the New Jersey (NJ) shoreline in October 2012.

The topography before and after Sandy as provided by USACE is used to assess the validity of the two vegetation modules.

The choice of the test site is based on two criteria, (1) the availability of pre-and post storm data of any historical storm over-washing the dune system and (2), the similarity of the vegetation to the RI shoreline, with the objective of adopting a reliable protocol and eventually apply the method in RI (where no data for storms in overwash regime are available). The model is first briefly described followed by a presentation of the selected scenarios. Data are described in the next section.

*3.1 Numerical Model*

XBeach ("eXtreme Beach behavior") is a 2-D coupled hydrodynamic and morphodynamic model that dynamically simulates the coastal response during time-varying storm conditions, and consequently the storm-induced changes in bed level (Roelvink et al., 2009, 2010). The model includes a choice of hydrodynamic models and a sediment transport model combined to a morphology change model. The model is designed to simulate processes occurring during the four erosion regimes defined by Sallenger (2000), swash, collision, overwash and inundation. The modeled coastal response includes dune erosion, breaching and accretion. In this work we use and compare results using two hydrodynamic modules, the Surfbeat and the Non-hydrostatic models. For both hydrodynamics approaches we use the two vegetation parameterizations. Each module of the XBeach model is briefly described hereafter.

*3.1.1 Surfbeat Mode (phase averaging)*

The "Surfbeat" model simulates mean currents in combination with a wave action conservation equation. The characteristic feature of this model is the modeling of the long

wave component of swash motions, the surf-beats resulting from the forcing by wave groups of infragravity waves and causing slow oscillations of the mean super-elevated water level (period of 20 to 250 sec) directly related to foreshore erosion (Longuet-Higgins and Stewart, 1964; Schaffer et al., 1993). Surf-beats are indeed particularly dominant in the surf zone in storm conditions, since the incident-wave frequency band (0:05 < f < 0:18 Hz) is saturated, while the infra-gravity frequency band is not, in particular on dissipative beaches (Raubenheimer et al., 1996). While the full directional distribution of wave action is maintained, the frequency spectrum is limited to a single frequency, the peak frequency. The propagation of wind waves is based on the conservation of wave action equation, coupled to a roller energy balance equation (Svendsen, 1984) in the surf zone through the wave dissipation term. Radiation stress tensors acting as forcing terms for depth- and period-averaged mean current equations are expressed based on linear wave theory. The mean current equations are the standard 2-D nonlinear shallow water equations expressed in a Generalized Lagrangian Mean formulation. Bottom shear stress terms are estimated based on the Eulerian velocity occurring at the seabed. The 2D depth-averaged equations are used to model the infragravity waves. The surf-beat approach has been validated on dissipative beaches with a surf similarity parameter ranging from 0 – 0.619 (dissipative beaches) (e.g. Van Rooijen et al. 2011; Nederhoff, 2014; Schambach et al., 2018; Elsayed and Oumeraci, 2017). Indeed on dissipative beaches the short waves are mostly dissipated by the time they reach the shoreline, and only infragravity waves reach the shoreline.

*3.1.2 Non-hydrostatic Mode (phase resolving)*

In Surfbeat mode, parametric functions are used to determine the nonlinear evolution

of wave fields, whereas in non-hydrostatic mode these are fully resolved. Instantaneous wave velocities and water level variations are captured within the nonlinear shallow water equations by including the non-hydrostatic pressure force. In this way the dependency on the wave action equation becomes redundant. The non-hydrostatic model is particularly applicable for reflective beaches, where short waves have more significant impact on beach erosion (Smit et al., 2010, 2013, 2014; Van Rooijen, 2011).

The numerical scheme used is as introduced by Stelling and Zejlima (2003), and further developed by Zejlima and Stelling (2008) which gives competitive predictions in shallow waters compared to higher order Boussinesq models (e.g. Chen et al. 2000), while only maintaining a single layer (Smit et al., 2010, 2013, 2014). By using an edge based finite method, and a momentum conservation scheme, the possibility to model wave breaking without using a separate model was shown. In XBeach, this was further developed by Smit et al. (2010) to include a limited version of a scheme introduced by MacCormack (1969) to allow for more accurate predictions of shock waves and breaking.

*3.1.3 Vegetation Module in XBeach*

The energy dissipation through drag and turbulence when waves are propagating across vegetation is modeled as a dissipation term, $D_v$, in the wave action equation [$\frac{\partial E c_g}{\partial x} = D_v$] is solved according to Mendez and Losada's (2004), with E, the energy density [E=(1/8)$\rho g H_{rms}^2$], $c_g$ the group velocity , $x$ the onshore coordinate and $g$, the gravitational acceleration.

$$D_v = \frac{1}{2\sqrt{\pi}} \rho C_D N b_v \left(\frac{gk}{2\sigma}\right)^3 \frac{sinh^3 k\alpha h + 3\sinh k\alpha h}{3k\, cosh^3 kh} H_{rms}^3 \quad (1.1)$$

with $D_v$ the time-averaged rate of energy dissipation per unit horizontal area induced by the vegetation, $C_D$ a depth-averaged drag coefficient, $\rho$ is the water density, $k$ the local wave number, $H_{rms}$ the root mean square wave height, $N$ the number of vegetation stem per unit of horizontal area, $b_v$ the plant area per unit height of each vegetation stem normal to the velocity, $\sigma$ the wave angular frequency, $\alpha$ the relative vegetation height (%) relative to the local water depth $h$.

The model can include layered vegetation (e.g., to represent heterogeneous vegetation, such as mangroves; Suzuki et al. 2011). In that case the dissipation term is simply the sum of several dissipation terms, each associated with specific layer. The model can also include the swaying motion of the vegetation, which requires a re-calibration of the drag coefficient (e.g. Maza et al., 2013).

*3.1.4 Bed Friction Parameterization*

The standard approach to account for the effect of vegetation on the flow velocity is using a spatially variable friction coefficient function of the bed roughness associated with the specific land cover (Kothyari et al., 1997; Van Rijn, 1989; Wamsley et al., 2009, 2010; Schambach et al., 2018). The Manning coefficient (n) can be expressed as (e.g., Wamsley et al., 2009):

$$n = \sqrt{\frac{{C_{bf}}^2 h^{1/3}}{g}} \quad (1.2)$$

where $C_{bf}$ is a bed friction coefficient, and h is the water depth. The value of the Manning coefficient is assigned according to land cover following Wamsley's e al.

(2009), as used in Schambach et al. (2018) and shown in Table 1.1. Other vegetation covers found at study site, where interpolated from this table (e.g. Herbaceous dunes).

*Table 1.1 – Recommended Manning "n" values for specific land cover types*

| **Land Cover Type** | **Manning Roughness "n" value** |
|---|---|
| Open Water | 0.020 |
| Low Residential | 0.070 |
| High Residential | 0.140 |
| Deciduous and Mixed Forests | 0.120 |
| Evergreen Forest | 0.150 |
| Shrub Land | 0.050 |
| Grassland | 0.034 |
| Woody Wetland | 0.100 |
| Herbaceous Wetland | 0.040 |

*3.1.5 Sediment Transport Module*

The sediment transport model used in this study is the default model in XBeach introduced by Van Rijin (2007) and further developed by Van Theil (2009) based on the depth-averaged advection-diffusion equation (Galappatti and Vreugdenhil, 1985). The sediment transport is controlled by the sediment concentration in the water column relative to an equilibrium concentration (Soulsby et al., 1997). While wave propagation equations are based on linear theory, the effect of non-linear waves on sediment transport is included by adding an arbitrarily parameterized advection velocity $u_a$ (Stokes drift) to the Eulerian velocity, based on a wave skewness $S_k$ and asymmetry $A_s$ parameters both weighted by arbitrary empirical coefficient, $f_s$ and $f_a$ (so called facua parameter) (Roelvink et al., 2010).

*3.1.6 Model Parameters*

Default model parameter values were used, except for cases where extensive sets of

validation and recommendations were provided through comparative field analysis and laboratory experiments (Nederhoff, 2014; Devet et al. 2015; Van Rooijen, 2011; Roelvink, 2009; Elsayed and Oumeraci, 2017; Schambach et al. 2018). In XBeach, these parameters are bed friction coefficients, wave skewness and assymetry "facua" parameter, morphodynamic accelerator factor "morfac", critical wet and dry slope avalanching values, and scaling factor "eps". Further sensitivity analyses of these parameters were also provided. XBeach is presented in detail in Roelvink et al. (2009, 2010, 2018).

[Note that we used XBeach version XBeachX 1.23.5446M), released with the fortran and MPI options]

*3.2 Simulation Scenarios*

At the test site we model the coastal impact of Superstorm Sandy (October 2012) using four different approaches based on the choice between the wave hydrodynamic module and the vegetation module as summarized in Table 1.2. For modeling wave hydrodynamics, both the Surfbeat and the Non-hydrostatic modules are tested in combination with either the vegetation parameterized with a Manning coefficient or modeled with the vegetation module based on Mendez and Losada's (2004) formulation.

*Table 1.2 – Simulation scenarios used in this study*

| **Scenario** | **Wave Hydrodynamic model** | **Effect of Vegetation** |
|---|---|---|
| 1 | Surfbeat *(long wave resolving)* | Manning Roughness Coefficient |
| 2 | Non-hydrostatic *(Short wave resolving)* | Manning Roughness Coefficient |
| 3 | Surfbeat *(long wave resolving)* | Vegetation module |
| 4 | Non-hydrostatic *(Short wave resolving)* | Vegetation module |

*3.2.1 Scenario 1 and 2*

In both of these scenarios the Manning Roughness approach is used to model the effect of vegetation on sediment transport. This allows comparison between the Surfbeat and Non-hydrostatic approach. The models are used in 2-D and the friction is spatially variable based on the vegetation cover found at the study site. Vegetation data is described in the next section. Assessment of the morphological performance of the model for both scenarios is determined using BSS and Bias Scores (Van Rijin et al., 2003) as well as the Root mean square error RMSE, when comparing model results with pre and post-survey measurements, in the form of sub-aerial eroded volume or post storm geomorphology.

*3.2.2 Scenario 3 and 4*

In both of these scenarios the vegetation module is used to describe the effect of vegetation on sediment transport. Additional numerical experiments are undertaken for scenario 3 and 4 to validate the implementation of Mendez and Losada's (2004) formulation in XBeach. The objective of these numerical experiments is to obtain a general understanding on how the sediment transport rate is affected by the vegetation module as compared to the Manning Approach. Results from these experiments and the field study are used to evaluate the performance and applicability of each scenario.

*3.3 Assessment and Evaluation Methods*

The ability of the model to simulate accurately the eroded volume is assessed by computing several skill parameters. A summary of the skill parameters used to assess the accuracy of the model for each scenario is presented in Table 1.3. Parameters are the Brier (BSS) and Bias (BI) scores, the Root Mean Square Error (RMSE), and the skill of

the model as defined by Gallager et al. (1998) (SK), and used in Schambach et al. (2018) that compares the relative value of the eroded volume.

*Table 1.3 – Summary of skill parameters used to assess the simulation results.*

| Statistical Skill Parameter | Conceptual assessment | Optimal value | Formulation |
|---|---|---|---|
| SK | Relative value of the eroded volume | 1 | $SK = 1 - \frac{\sqrt{\sum_{i=1}^{N}(V_c - V_o)^2}}{\sqrt{\sum_{i=1}^{N} V_o{}^2}}$ |
| BSS | Morphological skill to compute bed level change | 1 | $BSS = 1 - \frac{\sum_{i=1}^{N}\left(z_{b,comp} - z_{b,meas}\right)^2}{\sum_{i=1}^{N}\left(z_{b,initial} - z_{b,meas}\right)^2}$ |
| BI | Difference in central tendencies of computed and observation | 0 | $BI = \frac{1}{N}\sum_{i=1}^{N}\left(z_{b,comp} - z_{b,meas}\right)$ |
| RMSE | Accuracy of computed results | 0 | $RMSE = \sqrt{\frac{1}{N}\sum_{i=1}^{N}\left(z_{b,comp} - z_{b,meas}\right)^2}$ |

## 4. Site Description and Model Set-up

Hurricane Sandy (2012) was one of the most destructive storms to hit the US North Atlantic Coast to date. Estimated cost of damage was at least $50 billion as reported by the National Hurricane Center (Blake et al., 2013). Approaching its landfall location with a forward speed of 10 m/s and wind speed 38.5 m/s, it caused severe overwash, flooding and inundation along the coastlines of New York and New Jersey in particular (Blake et al., 2013). Many of the undeveloped sections of the barrier islands close to the landfall location left pampered after the incident.

In response to this event, the USGS in collaboration with National Oceanic and Atmospheric Agency (NOAA) and other state and federal agencies developed a database of the areas affected by Sandy, consisting of large scale aerial photographs, bathymetric and topographic LiDAR survey measurements, and land cover surveys. This data captured many of the morphological changes that occurred during the storm and is utilized for this study.

Figure 1.1 shows the chosen site, which is a 2 km stretch of barrier beach with an average width of 400 m. It is located 20 km north of the landfall location, and is made up of vegetated bed cover.

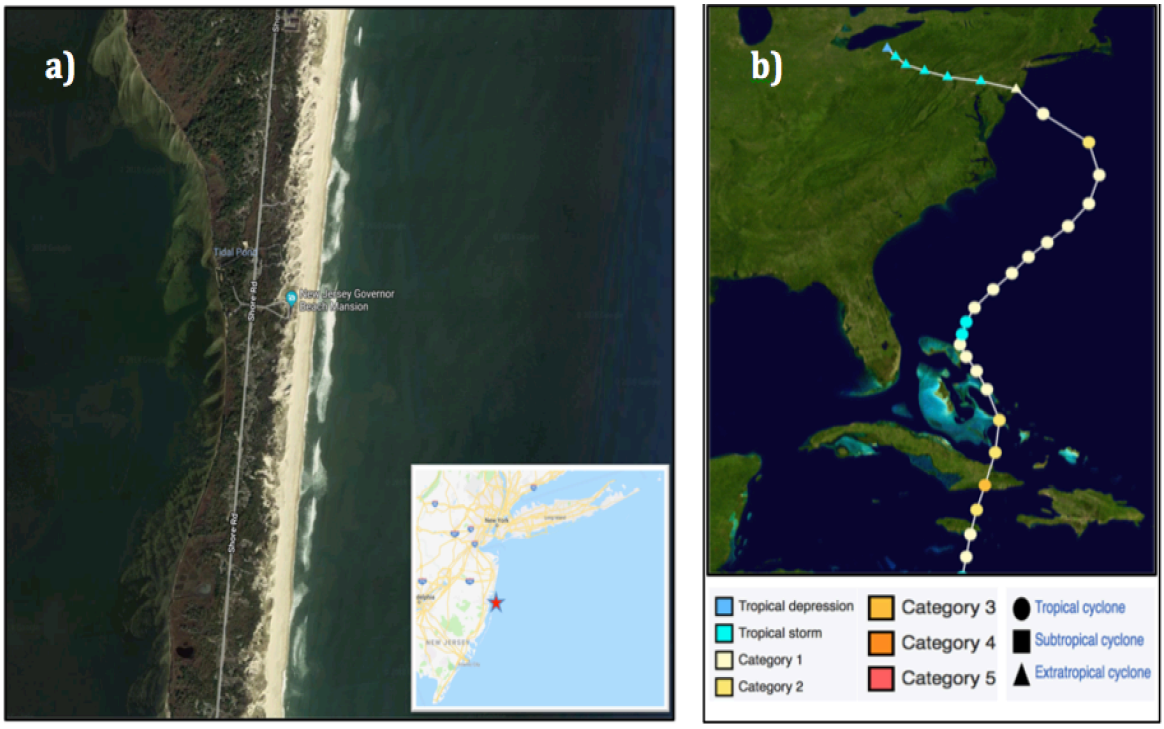


***Figure 1.1*** *Description of the study area and Hurricane Sandy 2012. a) Aerial Photograph of the selected site located in Ocean County, NJ south of Seaside Heights. Taken from Google maps 2018. b) Hurricane Sandy Track and storm category based on the Saffir-Simpson Scale, taken from NHC Report (Blake et al. 2013).*

*4.1 Pre and Post Survey Measurements*

Topography for the pre and post event was extracted from the NOAA DEM database developed as part of the National Assessment of Coastal Change Hazards. This data has a resolution of 2 by 2 m, and covers the entire subaerial dune topography and the backshore of the beach. Pre surveys were taken on August 2010, two years before the storm. Post surveys were taken in June 2013, 9 months after the storm. Despite the offset period between measurements and the time of the storm, no major changes were expected to have occurred since the site is undeveloped and is unaffected by human activities. In addition no storms occurred during this time except for hurricane Sandy, and the only morphological changes that may have occurred is likely, mostly due to aeolian transport, which is insignificant since it operates at larger time-scale.

Bed level change analysis on the data showed significant morphological changes between the two surveys similar to what was described in Morton et al. (2003) for a storm-varying regime. The averaged sediment erosion volume calculated from the measurements is around 150 $m^3$, indicating severe dune erosion, crest lowering, imbreachments, and overwash fans. These are presented in Figure 1.2.

*4.2 Vegetation and Land Cover*

The spatial variability of land cover and vegetation type was determined using the USGS land cover surveys (30m resolution) interpolated on our high resolution computational grid. Figure 1.3(a) provides a 2-D description of the site land cover. The distribution of vegetation is typical of barrier beaches on the North East Atlantic Coast, and identifies areas of mixed forests at the north region, as well as shrubs and wetlands behind the dunes. Data from USGS was not able to capture the sparse vegetation on top

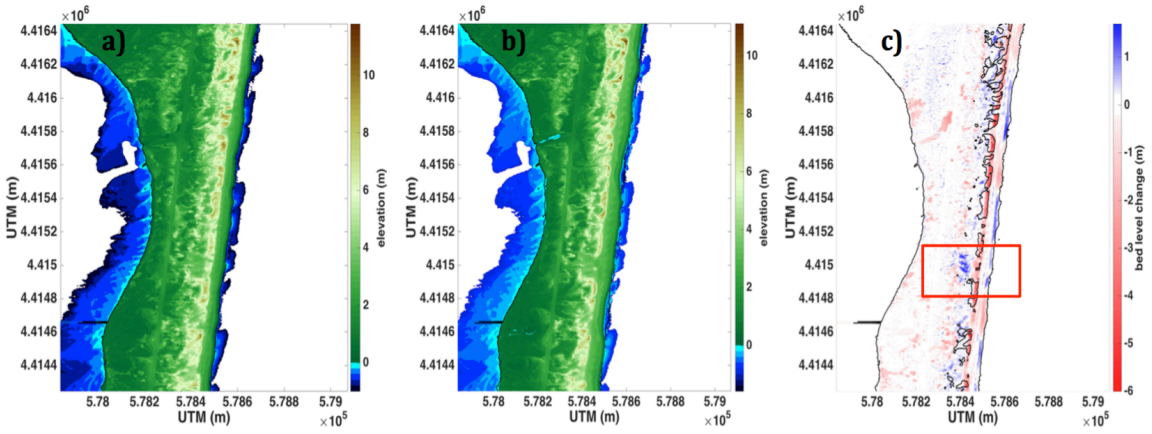


***Figure 1.2*** *Pre and post topographic survey measurement of Hurricane Sandy 2012. a) and b) are pre and post LiDAR survey measurements of the subariel topography and backshore of the beach using UTM horizontal coordinates and NAVD88 as vertical datum. c) Bed level change analysis between the two measurements. Contour lines show 0m, and 6m respectively of the pre sandy dune elevation. Red box showing location of dune imbreachment and the consequent overwash fan sediment deposition.*

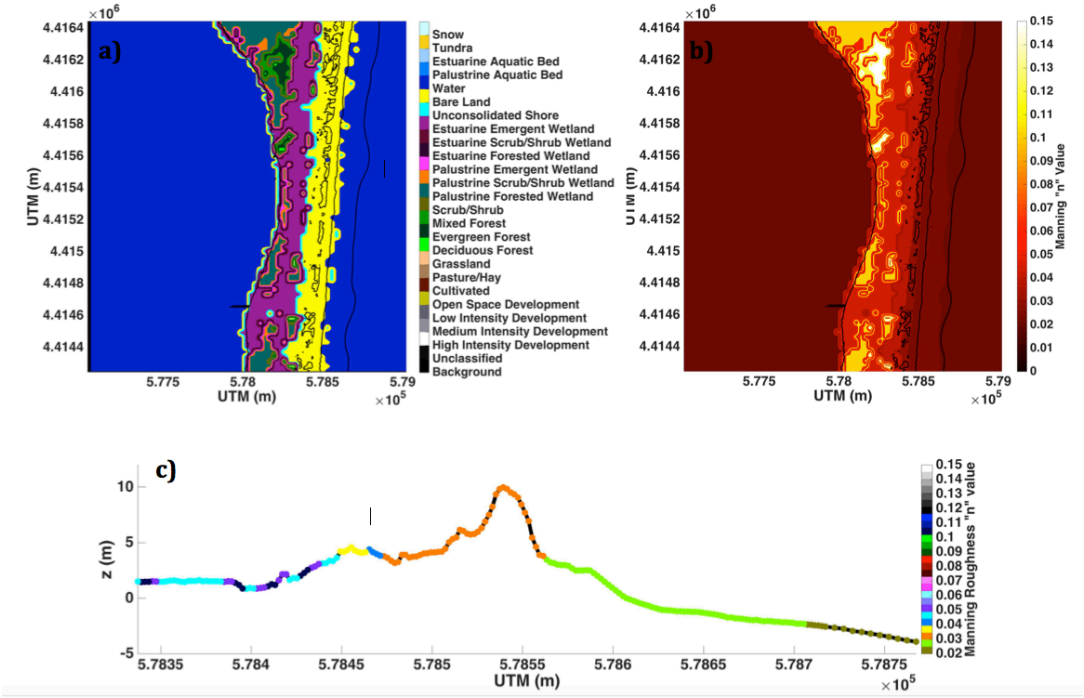


***Figure 1.3*** *Spatial description of land cover at the study site. a) Spatial distribution of land cover obtained from NOAA's website. b) Conversion of land cover to Manning roughness coefficient. Black contour lines are shown for, -4m, 0 m, 6 m referenced to NAVD88. c) Typical pre storm cross section with spatial distribution of land cover, showing gradual increase of Manning roughness. The right side is the seaward boundary and the left is the bay side.*

of the dunes. These were manually adjusted when converting the land cover type into Manning roughness as described in Section 3.1.4. Figure 1.3(b) shows the spatial distribution of Manning roughness (n) values as specified in XBeach simulations. Figure 1.3(c) shows a typical pre storm transect across the dune at the site (Fig. 1), showing a Manning coefficient varying progressively from 0.025 in the sandy beach foreface (green), to 0.03 when the herbaceous dunes appears (orange), to 0.05 in the shrub area in the back dune (blue), and finally to 0.035 when *Spartina Alterniflora* appears in the wetlands at the backside of the barrier (yellow).

*4.3 Computational Grid*

To construct a computational grid for XBeach, bathymetric data in the surfzone was required. These were obtained from the NOAA DEM database. The publication date of the data is December 2015, and therefore some uncertainty of the pre-storm bathymetry remains. These were combined with the topographic data described in section 4.1. The final grid has a resolution of 2x2m near the dune area, and 2x5m offshore and is shown in Figure 1.4.

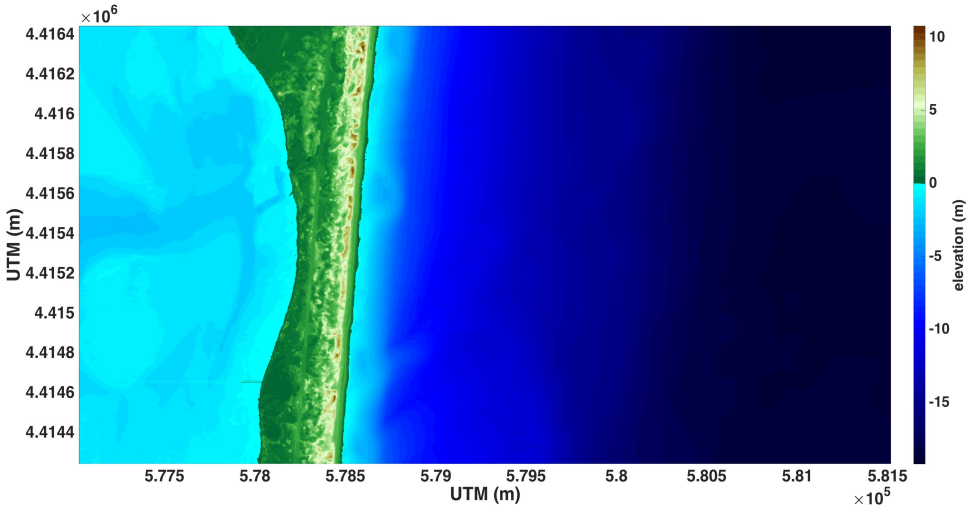


***Figure 1.4*** *Computational grid used to simulate Hurricane Sandy 2012 in XBeach.*

*4.4 Boundary Conditions*

The start date of the simulation was October 28, 2012 00:00:00 UTC, and the end date was October 31, 2012 00:00:00 UTC. The hydrodynamic boundary conditions i.e. waves and water levels were obtained from available simulation results of a coupled model (SWAN and ADCIRC) at the offshore boundary location. A peak significant wave height of $H_s$ = 6.5 m, spectral peak period $T_p$ = 16, mean direction θ = 170 degrees in nautical convention and a peak water level of 2.7 m were specified at the offshore boundary location of our computational grid during landfall. In addition water level was specified at the bay side from data at the USGS buoys. The entire duration of the simulation is 72 hours, with landfall occurring after 48 hours of simulations. Time series of the offshore boundary conditions are shown in Figure 1.5.

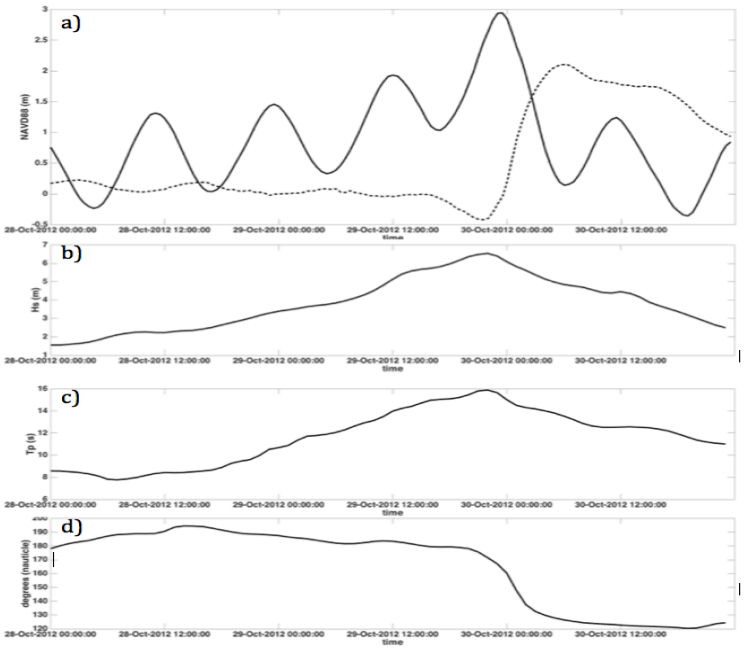


***Figure 1.5*** *Specified boundary conditions for hurricane Sandy at the study site location. a) Water level at Sea side (solid line) and bay side (dashed line) of the computational grid during simulation time. b) c) and d) are significant wave heights, peak period, and main angle of the incident waves respectively at the offshore boundary during the simulation time.*

## 5. Results

### *5.1 Results of Field Study for Scenario 1 and 2 Using Manning Approach*

Scenario 1 and 2 (Table 1.2) are compared to field survey measurements. In both cases the vegetation effect is modeled by a spatially variable Manning coefficient. In Scenario 1, the model is run in SurfBeat (SB) mode while in Scenario 2 the model is run in Non-Hydrostatic (NH) mode.

Both scenarios predicted the locations of the sensitive areas where the water surface elevation overtopped the dune and caused landward sediment deposition, similar to what was seen in the survey measurements. These areas are located in the southern region of the site, and consist of low dune elevation. Simulation results of Hurricane Sandy, indicate that the site experienced the three regimes of Sallenger in different sections of the barrier dune. Indeed the dune crest, which was relatively elevated in the northern section of the selected site, prevented overwash during the entire storm. As the dune crest was progressively lower in the southern area of the site, waves overtopped the dunes, which did not prevent overwash and inundation. This is illustrated by Figure 1.6, which shows the maximum water depth throughout the simulation for each location, identifying the regions that experienced overwash and consequently became inundated. Both scenarios gave similar prediction of these locations, however SB mode predicted higher maximum landward distance than NH mode. This however could not be validated since no water level measurements were taken. Therefore model performance will be based entirely on morphological predictions.

Comparison of simulation results and measurements indicates various morphological behaviors and sediment transport sequences occurring at different regions of the site.

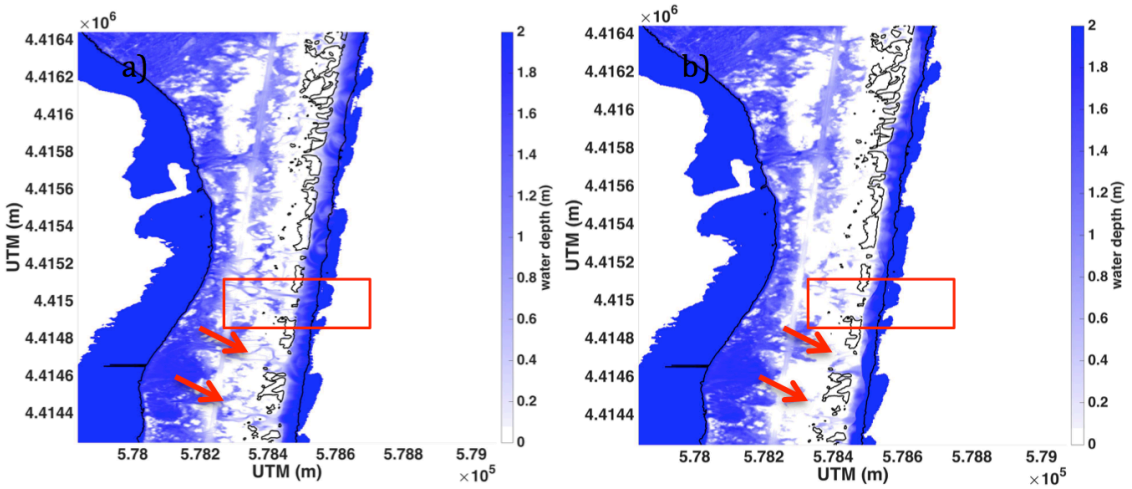


***Figure 1.6*** *Maximum water depths at each location during Hurricane Sandy showing areas, which were inundated during each simulation. a) and b) refers to Scenario 1 and 2 respectively. Contour lines are displayed for 0 and 6m. Red box shows location of overwash fan from measurements, and red arrows indicating regions where inundation regime occurred, causing landward sediment transport.*

The variation of the alongshore dune crest elevation allowed the site to experiences the three regimes of Sallenger, in different sections of the barrier dune. Areas with a consistently elevated dune crest prevented overwash during the entire storm, whereas regions with lower crest elevation let the waves overtopping the dunes, and did not prevent overwash and inundation. As a result intense erosion of the dune foreface occurred for areas experiencing a collision regime only in the northern part of the site, whereas dune erosion and landward deposition occurred for the areas in the southern part with lower dune elevation. This is further illustrated in Figure 1.7 which compares the alongshore dune crest elevations for both simulations with measurements, and shows areas that experienced crest lowering. Further illustration of the performance of each scenario is represented using 3 colors. Green indicates that the dune crest elevation was predicted with 0.5m accuracy or better. Yellow indicates locations experienced overwash and were predicted by XBeach, however the dune crest elevations have accuracy over

0.5m. Red indicates locations experienced crest lowering and were not predicted by XBeach. The total red dots were 106 and 201 for Scenario 1 and 2 respectively, indicating better performance with SB.

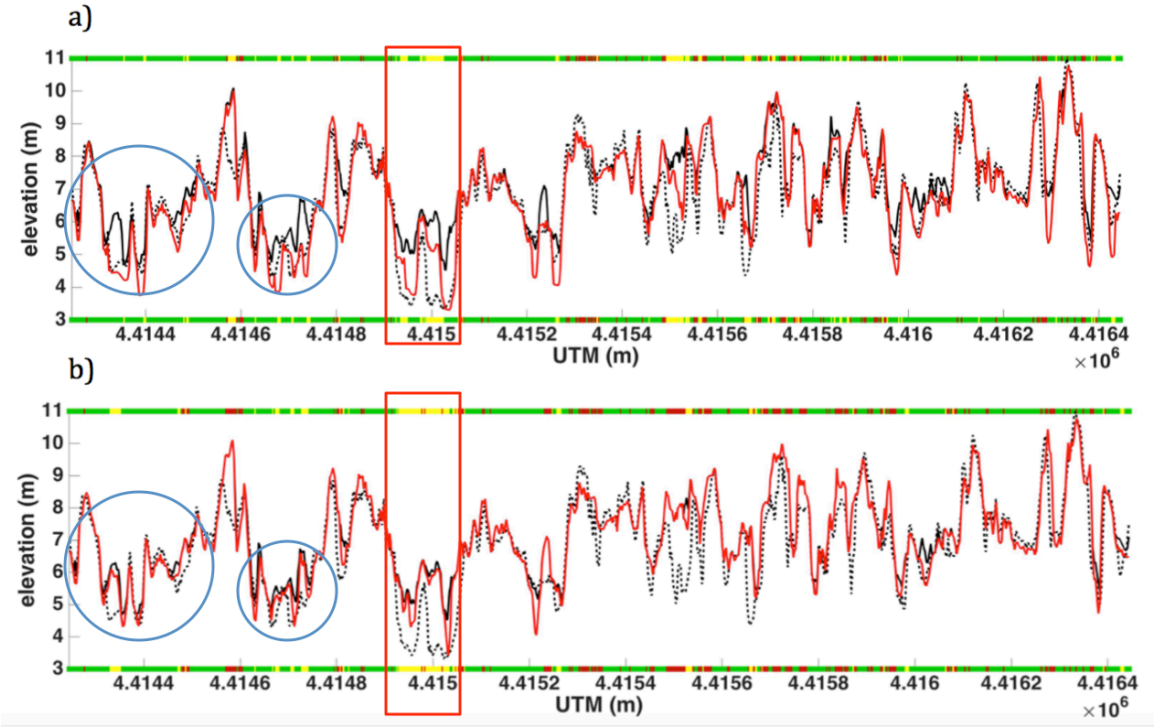


***Figure 1.7*** *Pre (solid black) and Post survey (dashed black) measurements of dune crest elevations are compared to XBeach simulatins (red line). a) and b) are re results for Scenario 1 (SB) and 2 (NH) respectively. Green shading indicates regions with 0.5m accuracy or better. Yellow shading indicates sections that experienced crest lowering but have discrepancy higher than 0.5m. Red shading indicates sections which experienced crest lowering but was not predicted by XBeach. Red box indicates location of overwash fan. Blue circles indicate other sensitive areas, which experienced overtopping at the south region of the site.*

Although Scenario 1 (SB) provides a better estimation of dune crest elevation and identification of sensitive locations than Scenario 2 (NH), the NH approach seems to predict more accurately than the SB approach the maximum water level and therefore the maximum landward distance of sediment deposition. This is illustrated in Figure 1.8,

which shows overestimation of the maximum landward distance for sediment deposition in SB mode as compared to measurements. This better representation of the maximum water level in NH mode is expected since, by definition in the NH mode, the hydrodynamic module is phase resolving and simulates the storm in real time while the SB mode is phase averaged. However, while the NH mode estimates well the sediment distribution pattern, it underestimates the eroded volume from the dune. At the opposite, the SB mode predicts a shorter deposition distance of the eroded sediment volume resulting in different sediment distribution patterns. Survey measurements show that erosion at sites experiencing a collision regime only, results in relatively less deposition in front of the dune foreface and beach foreshore than further offshore where most of the accretion occurs. By contrast, in areas experiencing overwash and inundation some sediment deposition can be observed on the beach foreshore. Though the uncertainty of the exact bathymetry after the storm however still remains questionable due to the time lag between the storm and post measurements.

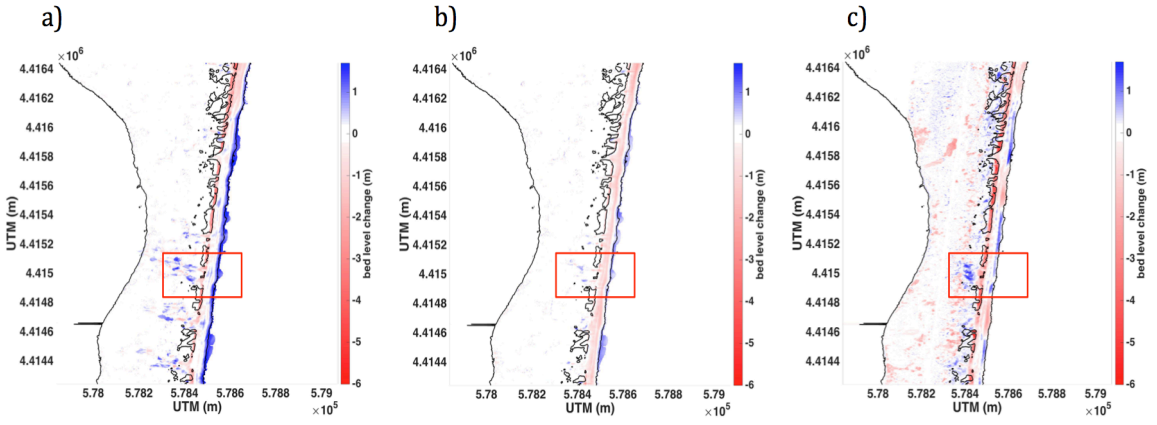


***Figure 1.8*** *Results of XBeach simulations for Hurricane Sandy 2012 showing final computed bed level changes. a) and b) refers to Scenario 1 (SB) and Scenario 2 (NH), whereas c) shows actual bed level changes from measurements. Red box indicate location of overwash fan. Contour lines are displayed for 0 and 6m.*

The ability of the model to simulate accurately the eroded volume is assessed applying Brier and bias scores at each grid cell (Figure 1.9) in the sub-aerial section of the dune. Let us note that unexpected significant pre-post storm discrepancies in topography were found inland in areas of dense vegetation due to a lack of filtering of the LiDAR data. These areas are relatively remote from the area of interest and excluded from the discussion.

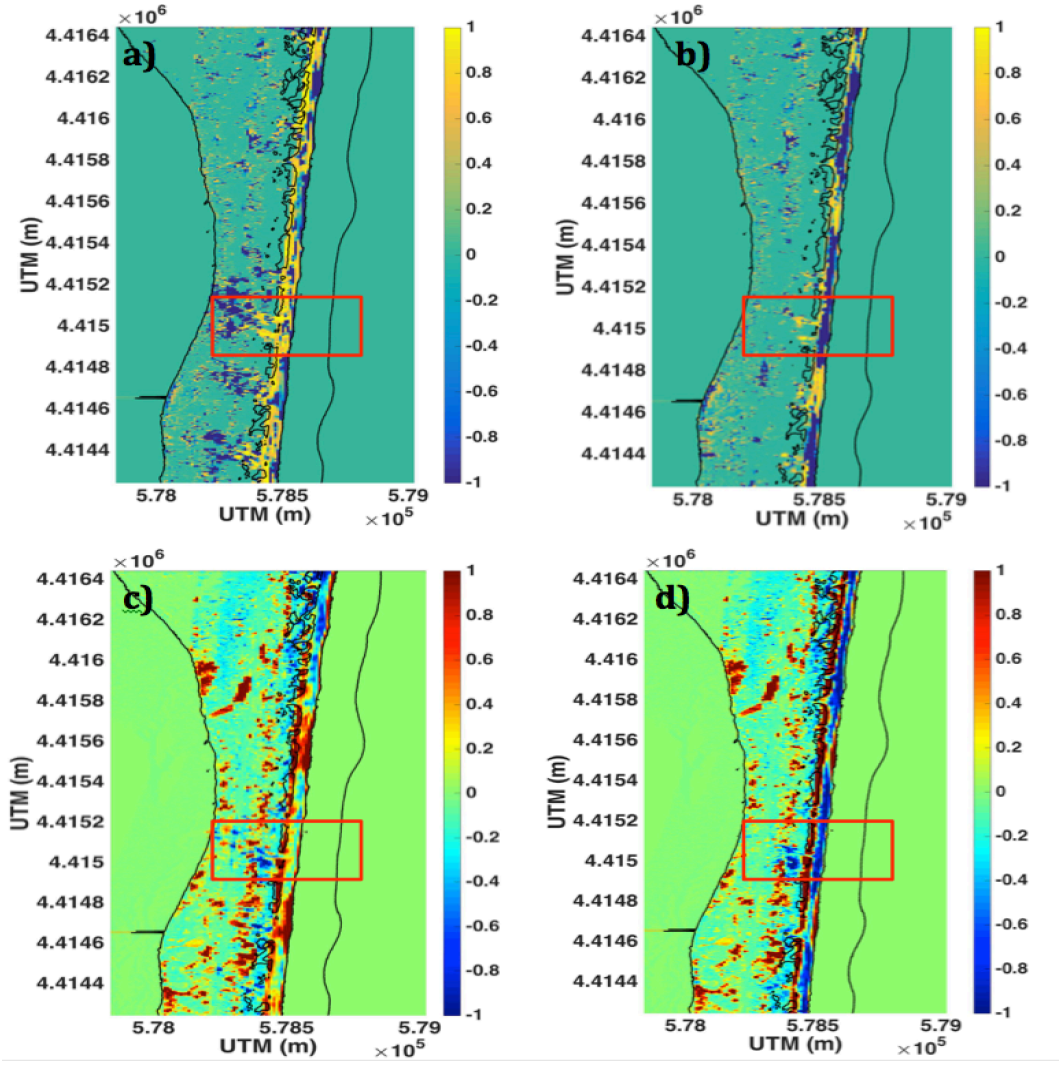


***Figure 1.9*** *Performance evaluation of the morphological predictions for both Scenario 1 (left panel) and Scenario 2 (right panel) using both BSS (top panel) and BIA (lower panel). Red box indicating area of overwash fan. Contours are displayed for -4, 0, 6m.*

The model performance was evaluated for three of Sallenger's regime, collision, overwash, and inundation. The site was further subcategorized into 3 areas, which were assessed separately. Since overwash and inundation regimes were prevented in the NH mode, its performance in the collision regime was evaluated and compared to the SB mode. The northern region having larger of dune elevations was subcategorized as Area A. The middle region, which experienced crest lowering but not landward sediment deposition was categorized as Area B. The southern part and the most sensitive part was categorized as Area C, is where overwash and inundation regime have occurred. The sub-categorization of the site is illustrated in Figure 1.10. A summary of the skill parameters of the model used to assess accuracy for each scenario and each subzone A, B, C is presented in Table 1.4, with the definition of these summarized in Table 1.3.

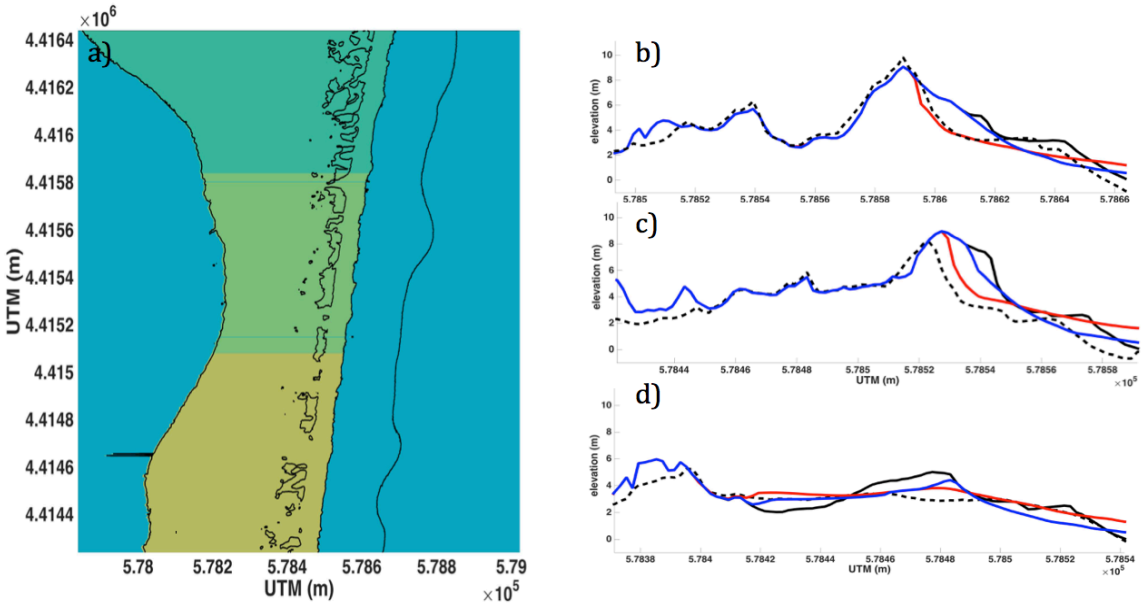


***Figure 1.10*** *Sub-categorization of the study site according to Sallenger's Regimes. a) Sub-categorization of site, Area A (top, dark green), B (middle, light green) and C (low, yellow) representing collision, over-wash and inundation regimes, respectively during Super-storm Sandy. Black contour lines are shown for, -4m, 0 m, 6 m referenced to NAVD88. a) b) c) showing cross sectional example for Area A, Area B, Area C respectively and compares SB results (red line), and NH (blue line) with pre (solid black) and post (dashed black) survey measurements.*

*Table 1.4 – Summary results of evaluation performance for Scenario 1 and 2 for Sallenger's regimes in the sub-aerial region*

| Scenario | Area A | | | | Area B | | | | Area C | | | |
|---|---|---|---|---|---|---|---|---|---|---|---|---|
| | SK | Mean BSS | Mean BI | Mean RMSE | SK | Mean BSS | Mean BI | Mean RMSE | SK | Mean BSS | Mean BI | Mean RMSE |
| 1 (SB) | 0.5 | 0.34 | 0.01m | 0.18m | 0.35 | -1.72 | 0.03m | 0.10m | 0.12 | 0.19 | 0.03m | 0.08m |
| 2 (NH) | 0.5 | 0.42 | 0.05m | 0.21m | 0.38 | 0.29 | 0.05m | 0.12m | 0.18 | -2.30 | 0.03m | 0.09m |

In Area A where the collision regime mainly dominated, both models showed a "reasonable" morphological skill according to Van Rijn et al. (2003) classification, with a BSS of 0.34 and 0.42 for SB and NH respectively. This was due to underestimation in the erosion rate on the foreface of the dune as indicated by the low SK value. In Area B, where crest lowering occurred and consequently overwash, NH mode showed a BSS of 0.29, while SB's BSS was -1.72. Since NH underestimated the erosion volume, and was restricting overwash regime; the corresponding BSS is for the collision regime. Although SB was able to predict the overwash regime in these areas, predictions were rated poorly. In zone C where inundation and landward sediment deposition occurred, SB gave better morphological predictions with a BSS of 0.19 as compared to -2.30 for NH mode. This region consists of lower dune elevations, which were wiped out during hurricane Sandy 2012. SB predicted elevation of dune crest lowering reasonably well as shown in Figure 1.7, however exact morphological profiles were not obtained. In NH dune crest elevation remained high during the simulation and prevented actual changes of the profile. The average results of each skill parameter for all zones are listed in Table 1.5.

*Table 1.5 – Average scores of each skill parameter for sub-aerial region including Area A, B, and C*

| Scenario | SK | BSS | BI | RMSE |
|---|---|---|---|---|
| 1 (SB) | 0.323 | -0.396 | 0.023m | 0.12m |
| 2 (NH) | 0.353 | -0.53 | 0.043m | 0.14m |

*5.2 Results for Scenario 3 and 4 using Vegetation Module in XBeach*

Prior to applying Scenario 3 and 4 to our field study better confidence and understanding on how sediment transport and dune erosion are affected by vegetation module, two numerical experiments were built for a coastline covered with *Spartina Alterniflora*. Various laboratory experiments were undertaken for this type of plant commonly found in wetland areas along the US North Atlantic coastline as described in Section 2.2. Information about this plant, and appropriate drag coefficients as suggested by these laboratory experiments will be used to perform these numerical experiments presented in this section.

*5.2.1 Numerical Experiment 1*

Both hydrodynamics modules, NH and SB, were ran using vegetation module in XBeach, and results were compared with Smith et al.'s results (2016) to verify the proper implementation of equation 1.1 in XBeach, and ensure reasonable estimation of the wave dissipation. In Smith et al. (2016) study, artificial vegetation to mimic the characteristics of *Spartina Alterniflora* was used in a flume experiment to determined a drag coefficient correlation which can be used in the Mendez and Losada's (2004) formulation. Using the calibrated drag coefficient, Smith et al. (2016) estimated the distance required by a vegetation field consisting of *Spartina Alterniflora* to dissipate 50% of the incident wave

heights.

A 1-D model was therefore constructed similar to a wave flume tank, but with a constant depth chosen to be relatively to the incident wave height. A vegetation field was applied at the bottom surface starting at 250m after the seaward boundary. The length of the vegetation field is 700m, and was chosen to be at least twice the wavelength of the maximum incident wave. A slope of 1:20 was specified at the landward side of the domain to dissipate incoming waves. Morphology and sediment transport modules in XBeach were turned off to simulate wave propagation and dissipation by vegetation only. A cross-sectional plot of the final model set up is shown in Figure 1.11. The physical characteristics of the plant are given in Table 1.6, and are similar to those used in the Smith et al. (2016). Simulation runs were for a combination of incident waves and relative depths as specified in the Smith et al. (2016).

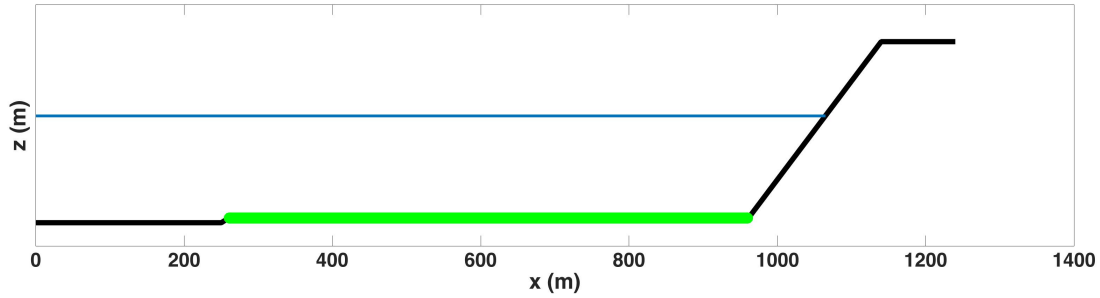


***Figure 1.11*** *1D model set-up for XBeach to calculate the distance required for Spartina Alterniflora to dissipate 50% of the incident wave height. Green shading refer to location of vegetation field. Blue line indicate still water level.*

*Table 1.6 – Physical Characteristics of Spartina Alterniflora used in XBeach*

| **Physical Characteristic** | **Value** |
|---|---|
| Stem Height | 0.415m |
| Stem Diameter ($b_v$) | 6.4mm |
| Density (N) | 400 stems/$m^2$ |

The value of the drag coefficient is estimated based on the correlation established with the Reynolds Number (Re) in Anderson and Smith's (2014) experiments (Smith et al., 2016). Smith et al., (2016) showed that $C_D = 910/Re + 0.22$, with a standard error of 0.034 for submerged vegetation; for emergent vegetation $C_D$ is about 25 to 20 % higher than for submerged vegetation.

Results are presented in Figure 1.12 in a non-dimensional formulation of the distance required to dissipate 50% of the wave height based on a relative water depth $k_p d$ versus $X50/L_p$, with $k_p$ and $L_p$ the peak wave number and wavelength respectively, d the water depth and X50 the distance across *Spartina Alterniflora* necessary to reduce the wave height by 50%. Wave height estimation are based on the maximum depth limited wave height as used by Smith et al. (2016): $Hmo_{max} = 0.1\ L_p \tanh(k_p d)$.

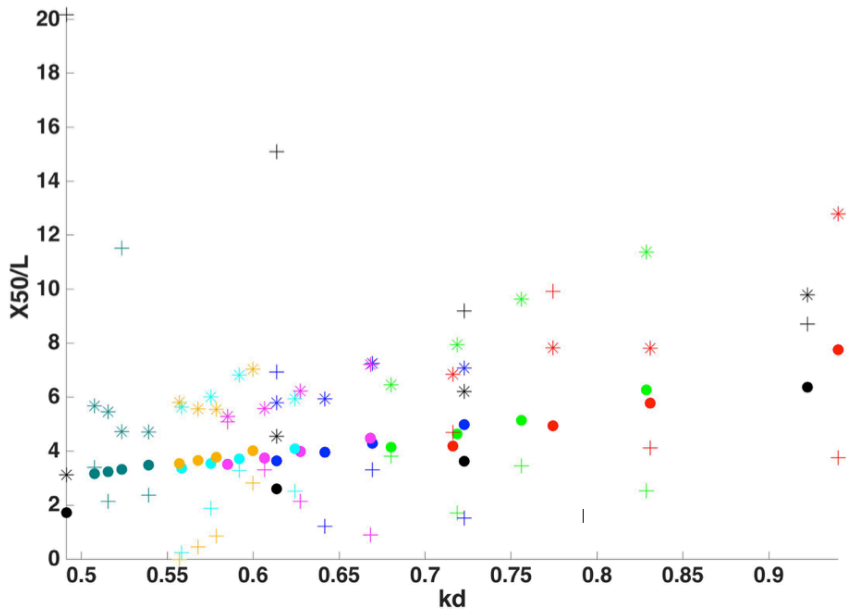


***Figure 1.12*** *Numerical experiment 1 results showing distance to 50% wave height reduction. Marker (o,*,+) refers to Smith et al. 2016, Surfbeat model, Non-hydrostatic. Colors refer to Incident wave periods (black=3s, red=4s, green=5s, blue=6s, magenta=7s, cyan=8s, yellow=10s, Dark green=12s)*

A similar trend to Smith's experiment, with however still some disparities: the SB mode systematically estimates more vegetated distance to limit the wave height while the NH predict that a shorter distance of vegetation can limit the wave height, and is therefore more sensitive to vegetation.

*5.2.2 Numerical Experiment 2*

In order to validate these approaches for modeling dune erosion during overwash and inundation regime, the results of a conceptual study is presented. In this study Scenarios 3 and 4, which uses the vegetation module in XBeach are compared with Scenario 1 and 2, which uses a parameterized friction coefficient. For this experiment Scenario 1 is considered as a baseline to assess results of the vegetation module, since it was found to give reasonable morphological predictions and estimation of dune crest elevation and erosion in Area C, which experienced inundation regime during Hurricane Sandy simulation (Table 1.4). A typical cross section of a barrier island covered with *Spartina Alterniflora* will be submerged under water for different depths and subjected to an incident wave with Hmo = 5m, $T_p$ = 10s. The correlation of the drag coefficient as presented in "Numerical Experiment 1" for this plant will also be used in this study.

To compare the approaches a Manning roughness coefficient was required to be selected. The "n" value selected for Spartina Alterniflora was 0.04, which was interpolated from Table 1.1. Furthermore, Yusof et al. (2017) gives a relationship between the drag coefficient and Manning coefficient for submerged vegetation. This relationship was also used to select an appropriate Manning roughness coefficient for this plant. Figure 1.13 gives a plot of all the results using a range of Manning roughness coefficients (0.04 – 0.15) to determine the sensitivity of the models to the this coefficient. The

vegetation module gave similar predictions to a Manning roughness of 0.15. This is however unlikely, since according to Wamsley et al. (2009) this roughness represents forests and wetland, and therefore have restricted morphological changes that could have occurred during inundation as suggested by the hurricane Sandy simulation.

To understand the reason behind the different predictions of sediment transport rates the velocities used for the sediment transport model described in Section 3.1.5 were compared. For the SB mode both the orbital velocity calculated from the wave action equation $u_{rms}$ and the depth average Generalized Langrangian Mean (GLM) velocities calculated from the non-linear shallow water equations are passed to the Van-Thiel-Van Rijin (2009) sediment transport model. In NH, orbital velocities are not calculated since the wave action equation is not used and only the depth averaged GLM velocities from are passed to the sediment transport model to determine the equilibrium sediment concentration.

This can be illustrated by comparing the Maximum GLM and orbital velocities that occurred at each relative depth. Figure 1.14 shows that in a relative depth close to zero (i.e. at the dune crest) whether using SB or NH, similar estimates of the maximum GLM velocities are obtained. When the dune crest is submerged (relative depth $< 0$), shortwaves are not completely dissipated, since the maximum values of the orbital velocities calculated from SB are shown to be significant. As a result, the NH estimates less erosion since the orbital velocities are not superimposed in the sediment transport module.

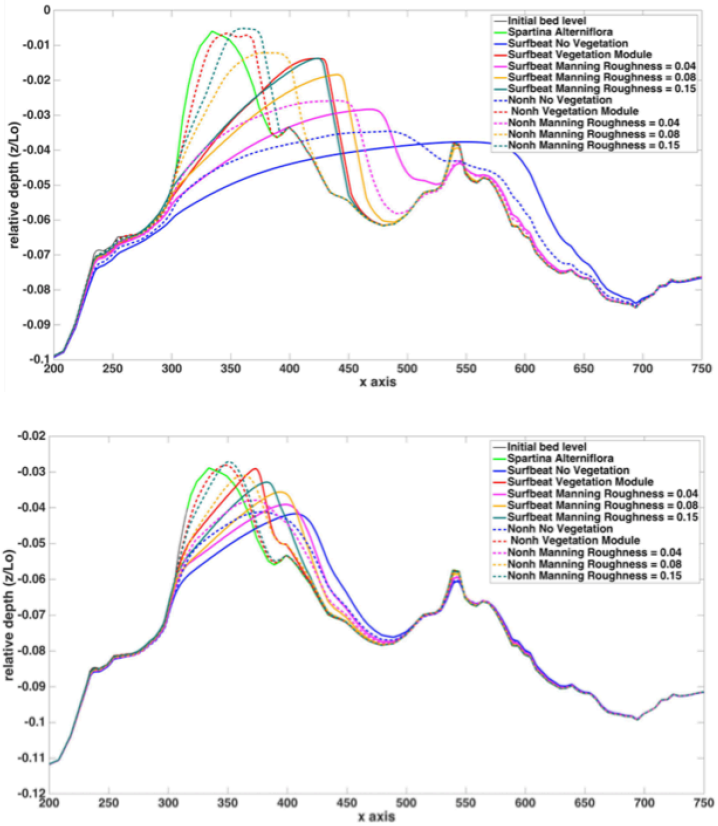


***Figure 1.13*** *Results of Numerical Experiment 2 showing bed level changes for two different depths using the vegetation module in XBeach for Scenarios 3 (solid red) and Scenario 4 (dashed red). Further comparison with manning roughness values "n" is provided (pink = 0.04, yellow = 0.08, dark green = 0.15, blue = 0.02 no vegetation), solid and dashed are for SB and NH respectively, black line and green shading refer to initial bed level and Spartina Alterniflora location.*

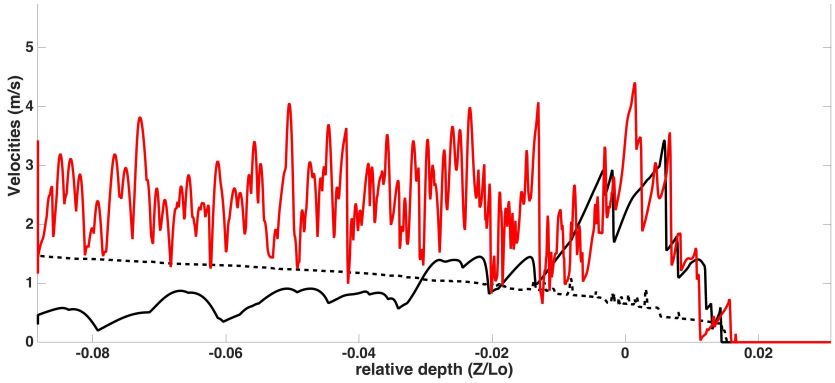


***Figure 1.14*** *Comparison of maximum velocities for Scenario 3 and 4 at depth. Red line indicating maximum GLM velocities for NH mode, where black line shows maximum GLM Velocities for SB. Dashed line refers to maximum orbital velocity in SB.*

*5.2.2 Application to Hurricane Sandy Simulation*

Numerical experiment 2 indicated that minimal dune erosion occurs when using the vegetation module in XBeach. However prediction from Scenario 3 and 4 could not be validated directly using the field data set on hurricane Sandy (2012), since it was not possible to apply it to the field study. This is due to lack of information on the physical characteristics of the vegetation, and more importantly, the drag coefficients for each vegetation type. Drag coefficient varies depending on the flow conditions and mechanical properties of the plant and limits the potential application of the vegetation module (Maza et al., 2013).

A more feasible way to determine the skill of the vegetation module is to scale up the Manning coefficients used to describe the vegetation field from hurricane Sandy simulation (Figure 1.3) to obtain similar predictions to that of the vegetation module. The scaled up Manning values will be used to run Scenario 3 and 4 and get the estimated erosion rates and ultimately bed level changes of the vegetation module. In Numerical experiment 2, it was seen that a Manning value of 0.15 instead 0.04 estimated similar dune erosion rate to using the vegetation module for both SB and NH. This suggests a scaling factor of 3.75 to be applied to the roughness values determined in the hurricane Sandy simulation in order to get similar results to what the vegetation module would predict.

Results for bed level change after hurricane Sandy simulations for Scenario 3 and 4 representing vegetation module predictions are presented in Figure 1.15. As stated, the vegetation module predicts less erosion at the dune crest where vegetation is presented. Although Scenario 3 was able to predict location of sensitive areas, Scenario 4 using the

NH did not. For Area A which experienced a collision regime only during sandy, and no vegetation interaction occurred, similar estimation of bed level changes was obtained for both SB and NH.

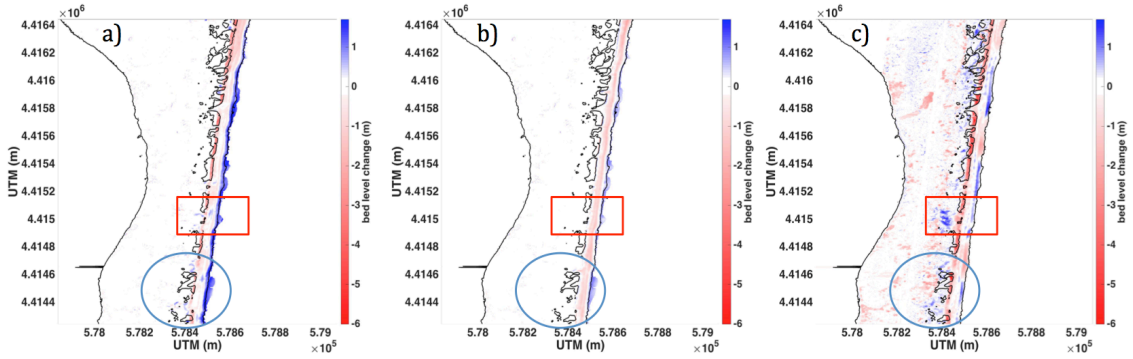


***Figure 1.15*** *Results of XBeach simulations for Hurricane Sandy 2012 showing final computed bed level changes. a) and b) refers to Scenario 3 (SB) and Scenario 4 (NH), whereas c) shows actual bed level changes from measurements. Red box indicate location of overwash fan, and blue circle indicating location of sensitive areas. Contour lines are displayed for 0 and 6m.*

Furthermore comparison of the dune crest elevation with survey measurements is shown in Figure 1.16. Red locations recorded were 105 and 293 for SB and NH respectively. When comparing the vegetation module predictions with Manning less accuracy of the dune crest elevation is obtained especially in the sensitive regions located in Area C. To compare the performance of predicting dune crest elevation for all scenarios, an index parameter is used. This index describes the ability of the model to well predict the dune crest elevation during an overwash storm regime. Further description of the index values are summarized in Table 1.7, where Table 1.8 presents the average index value for each scenario. Best scores were obtained for Scenario 1 when using the SB with Manning approach.

*Table 1.7 – Description of the performance indicator used to evaluate the estimation of dune crest elevations*

| Index value | Color | Description | Performance Indicator |
|---|---|---|---|
| 1 | Red | Did not predict locations of crest lowering | Poor |
| 2 | Yellow | Accurate prediction of dune crest lowering but with error greater than 0.5m. | Good |
| 3 | Green | Accurate prediction of dune crest lowering with error less than 0.5m. | Excellent |

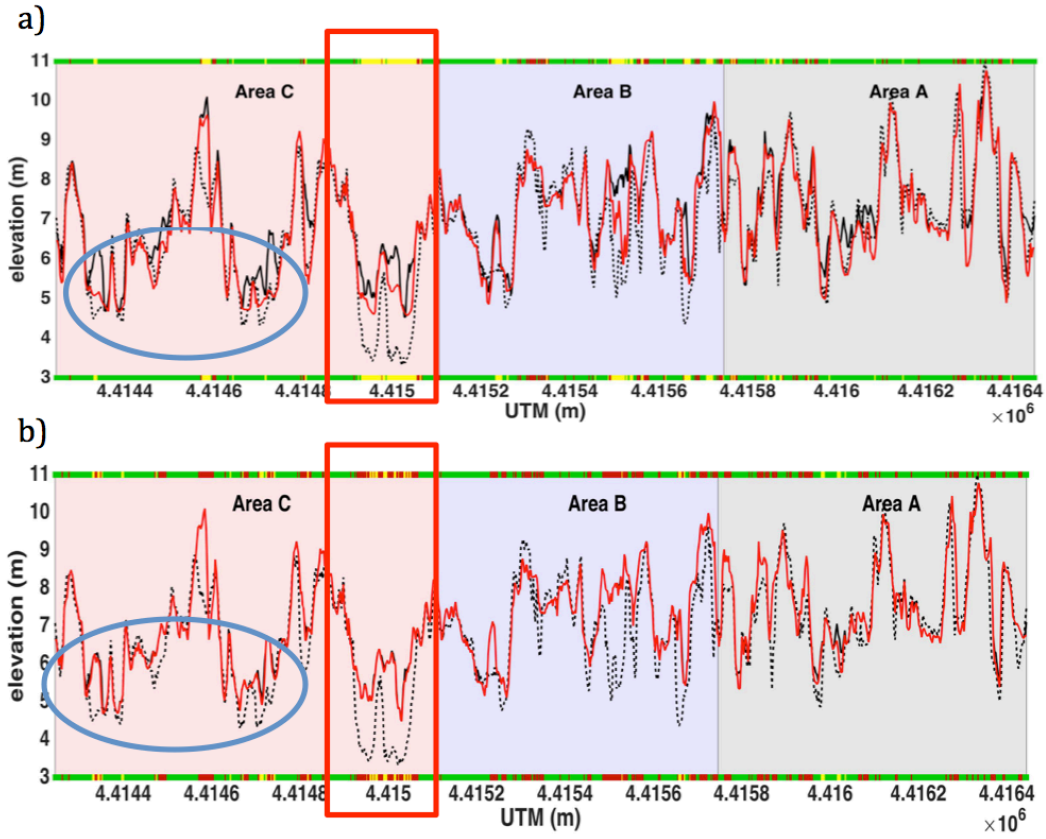


***Figure 1.16*** *Pre (solid black) and Post survey (dashed black) measurements of dune crest elevations are compared to XBeach simulations (red line). a) and b) are results for scenario 3 (SB) and 4 (NH) respectively. Green shading indicates regions with 0.5m accuracy. Yellow shading indicates sections that experienced crest lowering but have accuracy higher than 0.5m. Red shading indicates sections, which experienced crest lowering but was not predicted by XBeach. Red box indicates location of overwash fan. Blue circles indicate other sensitive areas which experienced overtopping at the south region of the site.*

*Table 1.8 – Summary of the average index values for predicting dune crest elevations*

| Scenarios | No. of Red locations | No. of yellow locations | No. of Green locations | Avg index |
|---|---|---|---|---|
| 1 | 106 | 133 | 695 | 2.63 |
| 2 | 201 | 123 | 610 | 2.43 |
| 3 | 105 | 154 | 675 | 2.61 |
| 4 | 293 | 61 | 580 | 2.30 |

A summary of the performance evaluation comparing all scenarios for Area A, B, and C is given in Table 1.9. Results show that vegetation module gave better BSS compared to Manning in Area A and B, which experienced collision and overwash respectively, but was very poor in Area C, which experienced inundation. When using the vegetation module with SB, better predictions of the eroded volume in Area A, B is obtained as indicated by the higher SK and BSS score. In Area C however, where the vegetation became submerged, the vegetation module predictions become poor. This can be further illustrated with a cross sectional examples comparing all scenarios for each area as shown in Figure 1.17.

*Table 1.9 – Summary of Performance evaluation for all Scenarios at Area A, B, and C*

| Scenario | Area A | | | | Area B | | | | Area C | | | |
|---|---|---|---|---|---|---|---|---|---|---|---|---|
| | SK | Mean BSS | Mean BI | Mean RMSE | SK | Mean BSS | Mean BI | Mean RMSE | SK | Mean BSS | Mean BI | Mean RMSE |
| 1 | 0.50 | 0.34 | 0.01m | 0.18m | 0.35 | -1.72 | 0.03m | 0.10m | 0.12 | 0.19 | 0.03m | 0.08m |
| 2 | 0.50 | 0.42 | 0.05m | 0.21m | 0.38 | 0.29 | 0.05m | 0.12m | 0.18 | -2.30 | 0.03m | 0.09m |
| 3 | 0.51 | 0.46 | 0.0095m | 0.18m | 0.39 | 0.35 | 0.03m | 0.096m | 0.17 | -2.27 | 0.03m | 0.07m |
| 4 | 0.5 | 0.47 | 0.05m | 0.22m | 0.38 | 0.34 | 0.05m | 0.11m | 0.16 | -2.23 | 0.03m | 0.09m |

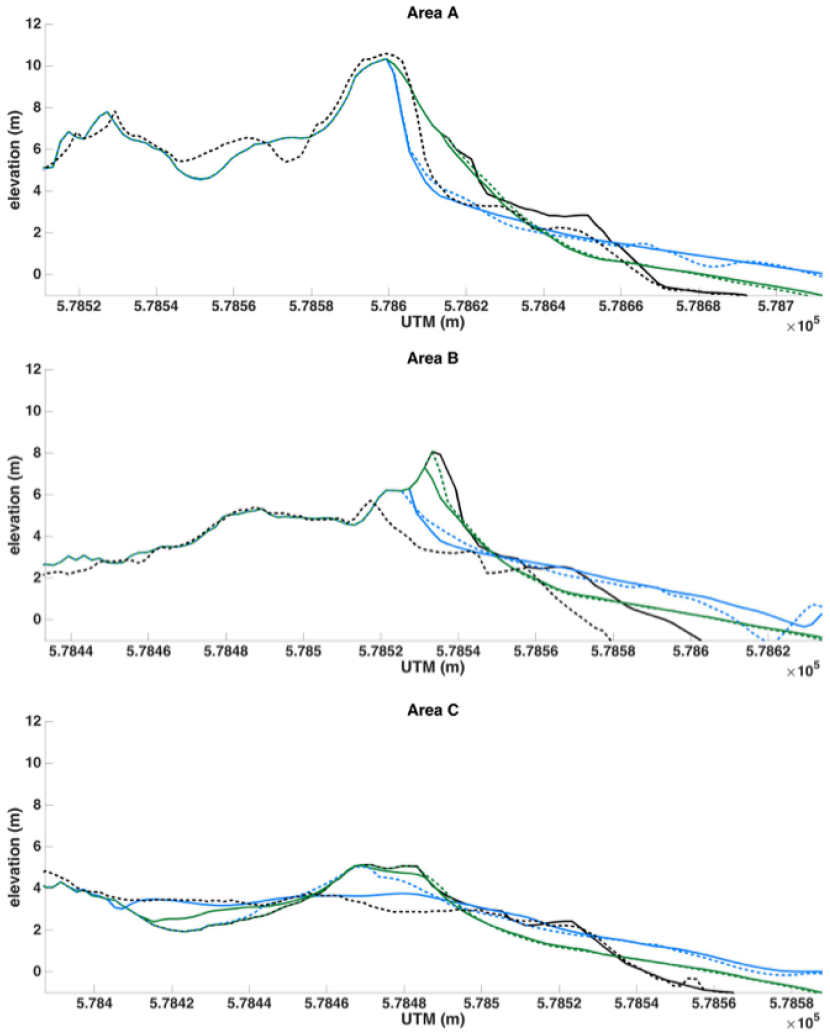


***Figure 1.17*** *Examples of Cross sectional profile after Hurricane Sandy Simulation for Areas experiencing collision, overwash, and inundation. Pre (solid black) and Post (dashed black) survey measurements are compared with Scenario 1 (solid blue), Scenario 2 (solid green), Scenario 3 (dashed blue), Scenario 4 (dashed green).*

## 6. Discussion

The results of this study allowed us to explore the performance of 4 different approaches to modeling the effect of vegetation on sediment transport and dune erosion during the 3 storm regimes identified by Sallenger (2000). Significant differences were found when these approaches were compared for each regime. In this section the sensitivity to both wave model and vegetation model are discussed for each storm

regimes. Further elaboration on the models capabilities and limitations are provided.

*6.1 Performance Assessment based on Storm Regime*

*6.1.1 Collision Regime*

The ability of XBeach to model the morphological changes of beaches, barrier islands, and dunes have been well validated for collision regime through laboratory and field experiments (e.g. Roelvink 2009, 2010; Schambach et al., 2018; Nederhoff, 2014; De Vet et al., 2015; Elsayed and Omeraci 2017). All scenarios gave competitive scores for Area A with the lowest BSS rated as “reasonable”. It must be noted also that discrepancies between the pre and post survey measurements were noticed in the vegetated areas due to filtering errors. It is therefore expected that these errors lead to much lower BSS and SK values.

Sensitivity to the wave model showed that better morphological predictions of the dune profile is obtained when using SurfBeat. Although this cannot be interpreted from the evaluation assessment since the NH gave better BSS and SK, it is clearly illustrated in Figure 1.17, which provides a cross-sectional example of the post dune profile for Area A. The NH predicts less dune erosion and avalanching, while SB show more accurate predictions. The lower BSS for the SB mode is a result of the large amount of sediment deposition occurring on the dune foreface zone. More accurate velocities in the NH mode lead to better alongshore and sediment distribution pattern of the eroded material, and further offshore deposition; hence overall better skill scores. This was further noticed when applying Scenario 3 and 4, where the vegetation module restricted dune erosion and hence sediment deposition resulting in better morphological skill, while the profile shape and crest elevations of the dunes were poorly predicted.

*6.1.2 Overwash Regime*

An important skill required for a model to predict flooding events is the capability to accurately estimate the dune crest elevation during a storm regime. This feature is most dominant when applying Scenario 1, which showed highest performance index for predicting dune crest elevation. Again since higher eroded volume occurred in Area B due to overwash, more deposition occurred in front of the dune leading to lower BSS. Nevertheless, the post-storm dune profile shape and crest elevations from Scenario 1 were the most accurate.

Despite more accuracy in water level, NH mode underestimates the eroded volume in collision and overwash modes. While it simulates well the landward transport distance of sediments in the over-wash regime, the volume is underestimated leading to a crest elevation remaining too high, which further restricts overtopping, and overwash. This was further observed when applying Scenario 3, and 4 that predicted less dune crest elevation, resulting in a lower index score when compared to Scenario 1 and 2 respectively (Table 1.8), and consequently less flooding and landward sediment transport.

*6.1.3 Inundation Regime*

Area C showed to be the most sensitive region with low dune crest elevation. Many of these areas became inundated and extreme morphological changes occurred. Best morphological predictions were obtained when using SB with a Manning roughness value as suggested by Wamsley et al. (2009). This has resulted in better BSS and estimation of landward sediment deposition volume compared to other scenarios. In addition the dune crest elevation was predicted with very good accuracy and an overall performance index of 2.63. All other scenarios failed to accurately predict the rate of

dune erosion, and therefore landward sediment transport leading to inaccurate morphological profile predictions and “poor” BSS.

*6.2 Performance Assessment based on Model Selection*

*6.2.1 Vegetation Module in XBeach*

The sensitivity of sediment transport to the vegetation formulation introduced by Mendez and Losada (2004) were explored through Numerical Experiment 1 and 2. In Numerical Experiment 1 confidence of the hydrodynamic conditions and wave propagation across a vegetation field were obtained when XBeach results showed similarities to Smith et al. (2016) study. In which, the suggested distance required to dissipate 50% of the incident wave heights were predicted by XBeach.

While the kinematic and dynamic free surface conditions in the presence of vegetation are well described when using the vegetation module in XBeach, the sediment erosion rates were not. The presence of vegetation results in a nonlinear modulation to the velocity profiles (e.g. Mazda et al., 2013; Vargas-Luna et al., 2015). Since XBeach computational grid consist of a single layer in the vertical direction, the nonlinearity of the depth velocity profile is not resolved, and is assumed to be linear. Hence, when integrating the velocity profile to calculate the depth-averaged velocities that are used in the sediment transport module, a significant reduction is introduced leading to much lower estimation of the sediment transport rate.

The vegetation formulations implemented in XBeach and described in Section 3.1.3 assumes rigid cylindrical structures and neglects the sway motion of the plant. For XBeach this is seen to be ideal, since the computational grid consists of a single vertical layer, and hence it is not possible to resolve the oscillatory deformation of the plant. More

profound equations were introduced which accounts for the displacement of the plant (Dupont et al., 2010). These are used to calculate the relative velocity between the water particle and the plant stem and determine an appropriate drag coefficient. Thus, plants with flexible stems will have lower relative velocity, and hence smaller drag (e.g. Stratigaki et al., 2011; Mendez et al., 1999; Maza et al., 2013). Mazda et al. (2013) showed that when the formulation is extended to include the sway motion of plant, the correlation of "bulk drag coefficient" becomes different than when no swaying. In the case of swaying, the drag increases compared to no swaying.

The sensitivity of these equations to the changing flow regimes during a storm event is not considered in which, only a constant drag coefficient value is chosen based on the average flow regime during a storm. In such case the evolution of the storm regime becomes restricted. As a result better predictions were obtained during collision in where the vegetation module restricted the overestimation of dune eroded volume in SB mode, but prevented overwash and inundation in the same time.

*6.2.2 Bed Friction Parameterization*

Scenario 1 and 2 gave best performance in overwash and inundation when using the Manning roughness coefficients suggested by Wamsley et al. (2009). In addition the estimated dune eroded volume and the landward sediment deposition volume were accurately predicted by Scenario 1 in the inundation regime. The capability of the Manning roughness to describe the sediment concentration has also been well validated in other studies (e.g. Schambach et al., 2018, Nederhoff, 2014). When using Manning roughness less energy dissipation is introduced to the profile if compared to the vegetation module and therefore higher depth average velocities leading to better

sediment concentration estimation. However this doesn't necessarily mean that accurate wave propagation was obtained when using the Manning approach, since higher land ward distance of sediment deposition occurred in areas experiencing inundation.

*6.2.3 Non-hydrostatic mode*

Low performance was observed when using the Non-hydrostatic mode, mainly related to underestimation of the erosion volume, which restricts development of the storm regime. Although results indicated good sediment distribution patterns and maximum landward distance of sediment deposition; hence accurate predictions of flow velocities; limitation of this module remains with the default sediment transport implemented in XBeach and used for this study as described in Section 3.1.5. The VanThiel-VanRijin (2009) sediment transport model uses the depth averaged GLM and orbital velocities $u_{orb}=u_{rms}$ to calculate the equilibrium sediment concentration of the water column. However, since the wave action is not used in Non-hydrostatic, the orbital velocities $u_{rms}$ are not calculated and only the GLM velocities are passed to the sediment transport model resulting in lower erosion and bed level changes. Numerical Experiment 2 suggested that $u_{rms}$ values are dominant during inundation and lead to higher estimation of dune erosion when using SB. While the effect of orbital velocities on sediment concentration is neglected in NH, this leads to significant errors. During a storm, the water depth increases significantly due to storm surge, wave set up, and bed erosion. The surfzone therefore becomes unsaturated and breaking occurs closer to the dune. In such event the dominancy of short wave instantaneous velocities dominate and cant be neglected.

*6.2.3 Surfbeat mode*

The main capability of Surfbeat is to simulate bed level changes and morphological changes of dunes, and barrier islands during Sallenger's Storm regimes in a feasible fashion. It remains the only model to accurately predict the dune crest elevations in the sensitive areas of our site. Using the recommended parameters suggested by literature and described in Section 3.1.6 proved to show reasonable results. Although the seaward deposition of the dune eroded volume is not accurately simulated, due to unresolved phase velocities. Comparison of simulation results and measurements indicate that further offshore deposition occurred of the eroded volume. Inaccurate predictions of sedimentation pattern in front of the dune, has therefore leading to lower performance scores.

**7. Conclusion**

The functionality of a dune system to protect coastal communities against hurricanes and seasonal storms, lead US federal and state agencies to assess the sustainability of these structures. Particularly in Rhode Island, dune crest elevation remains the major factor to reduce damage levels associated with flooding and overtopping during overwash and inundation storm regimes (e.g. Grilli et al., 2017a, 2017b; Spaulding et al., 2016, 2017; Small et al., 2016). Further studies on climate change and sea level rise scenarios indicated severe dune erosion may occur during a 100 year storm event, leaving many coastal communities vulnerable to austere environments (Schambach et al., 2018). Except for areas of dense vegetation, these showed more stability of the dune system.

Recent formulations describing the energy dissipation rate due to vegetation created more profound ways to model sediment transport in vegetated areas. The lack of

comparative analysis with field data sets however, remains uncertain and questions the reliability of these models. This study evaluated the performance of 4 scenarios to modeling the effect of vegetation on sediment transport and dune erosion during Sallenger's (2000) storm regimes. Combination of wave models and vegetation models were used to simulate the morphological changes occurred at the study site during Hurricane Sandy (2012). The capability and limitation of each scenario to model collision, overwash and inundation regime were identified when compared to pre and post storm measurements of the bed level.

Sensitivity to wave models indicated better performance when using the long wave resolving model in XBeach. Scenarios using "Surfbeat" mode led to overall better prediction of the post dune profile shape and crest elevation allowing the development of the storm regimes. Offshore and landward deposition distances however where inaccurately estimated leading to low performance scores. These were better predicted when using the wave-resolving model. Although, incompatibility of the default sediment transport model implemented in XBeach did not allow proper assessment of the Non-hydrostatic mode.

Depth averaging introduced large modulation errors to the GLM velocities when using the vegetation module in XBeach. While vegetation formulations simulates well the wave energy dissipation, and hence wave propagation, using them explicitly for modeling sediment transport resulted in poor performance scores. Manning roughness underestimates the wave dissipation, and predicts higher depth average velocities eventually leading to better morphological predictions.

In conclusion, Scenario 1 showed to be the most applicable approach for evaluating

the stability of a dune system during the storm regimes. Dune crest elevations can be accurately predicted by proper calibration of the model. Such feature makes it a feasible assessment tool for determining dune stability and identifying vulnerable areas.

**References**


Aburto, M.O., De Los Angeles Carvajal, M., Barr, B., Barbier, E.B., Boesch, D.F., Boyd, J., Crowder, L.B., Cudney-Bueno, R., Essington, T., Ezcurra, E. and Ganey, S., 2012. *Ecosystem-based management for the oceans*. Island Press.

Alongi, D., 2009. *The energetics of mangrove forests*. Springer Science & Business Media.

Andersen, K.H., Mork, M. and Nilsen, J.E.Ø., 1996. Measurement of the velocity-profile in and above a forest of Laminaria hyperborea. *Sarsia*, *81*(3), pp.193-196.

Anderson, M.E., Smith, J.M. and McKay, S.K., 2011. *Wave dissipation by vegetation. Coastal and hydraulics engineering technical note ERDC*. CHL CHETN-I-82. US Army Engineer Research and Development Center, Vicksburg, MS.

Anderson, M.E. and Smith, J.M., 2014. Wave attenuation by flexible, idealized salt marsh vegetation. *Coastal Engineering*, *83*, pp.82-92.

Arcement, G.J. and Schneider, V.R., 1989. Guide for selecting Manning's roughness coefficients for natural channels and flood plains.

Asano, T., Deguchi, H. and Kobayashi, N., 1993. Interaction between water waves and vegetation. In *Coastal Engineering 1992* (pp. 2709-2723).

Augustin, L.N., Irish, J.L. and Lynett, P., 2009. Laboratory and numerical studies of wave damping by emergent and near-emergent wetland vegetation. *Coastal Engineering*, *56*(3), pp.332-340.

Baldock, T.E., Holmes, P., Bunker, S. and Van Weert, P., 1998. Cross-shore hydrodynamics within an unsaturated surf zone. *Coastal Engineering*, *34*(3-4), pp.173-196.

Barbier, E.B., Koch, E.W., Silliman, B.R., Hacker, S.D., Wolanski, E., Primavera, J., Granek, E.F., Polasky, S., Aswani, S., Cramer, L.A. and Stoms, D.M., 2008. Coastal ecosystem-based management with nonlinear ecological functions and values. *science*, *319*(5861), pp.321-323.

Booij, N., 1981. Gravity waves on water with non-uniform depth and current.

Blake, E.S., Kimberlain, T.B., Berg, R.J., Cangialosi, J.P. and Beven Ii, J.L., 2013. Tropical cyclone report: Hurricane sandy. *National Hurricane Center*, *12*, pp.1-10.

Charnock, H., 1955. Wind stress on a water surface. *Quarterly Journal of the Royal Meteorological Society*, *81*(350), pp.639-640.

Chen, Q., Kirby, J.T., Dalrymple, R.A., Kennedy, A.B. and Chawla, A., 2000. Boussinesq modeling of wave transformation, breaking, and runup. II: 2D. *Journal of Waterway, Port, Coastal, and Ocean Engineering*, *126*(1), pp.48-56.

Cooper, Nicholas J. "Wave dissipation across intertidal surfaces in the Wash tidal inlet, eastern England." *Journal of Coastal Research* (2005): 28-40.

Dalrymple, R.A., Kirby, J.T. and Hwang, P.A., 1984. Wave diffraction due to areas of energy dissipation. *Journal of Waterway, Port, Coastal, and Ocean Engineering*, *110*(1), pp.67-79.

De Vet, P.L.M., McCall, R.T., Den Bieman, J.P., Stive, M.J. and Van Ormondt, M.A.A.R.T.E.N., 2015. Modelling dune erosion, overwash and breaching at Fire Island (NY) during Hurricane Sandy. In *The Proceedings of the Coastal Sediments 2015*.

Dubi, A. and Tørum, A., 1995. Wave damping by kelp vegetation. In *Coastal Engineering 1994* (pp. 142-156).

Dupont, S., Gosselin, F., Py, C., De Langre, E., Hemon, P. and Brunet, Y., 2010. Modelling waving crops using large-eddy simulation: comparison with experiments and a linear stability analysis. *Journal of Fluid Mechanics*, *652*, pp.5-44.

Elsayed, S.M. and Oumeraci, H., 2017. Effect of beach slope and grain-stabilization on coastal sediment transport: An attempt to overcome the erosion overestimation by XBeach. *Coastal Engineering*, *121*, pp.179-196.

Gacia, E. and Duarte, C.M., 2001. Sediment retention by a Mediterranean Posidonia oceanica meadow: the balance between deposition and resuspension. *Estuarine, coastal and shelf science*, *52*(4), pp.505-514.

Galappatti, G. and Vreugdenhil, C.B., 1985. A depth-integrated model for suspended sediment transport. *Journal of Hydraulic Research*, *23*(4), pp.359-377.

Gallagher, E.L., Elgar, S. and Guza, R.T., 1998. Observations of sand bar evolution on a natural beach. *Journal of Geophysical Research: Oceans*, *103*(C2), pp.3203-3215.

Grilli, A.R., Spauding, M.L., Schambach, L., Smith, J. and Bryant, M., 2017a. Comparing Inundation Maps Developed Using WHAFIS and STWAVE: A Case Study in Washington County, RI. *Proceeding of the ASCE conference: Coastal Structures and Solutions to Coastal Disasters 2015: Resilient Coastal Communities* .

Grilli, A., Spaulding, M.L., Oakley, B.A. and Damon, C., 2017b. Mapping the coastal risk for the next century, including sea level rise and changes in the coastline: application to Charlestown RI, USA. *Natural Hazards*, *88*(1), pp.389-414.

Holthuijsen, L.H., Booij, N. and Herbers, T.H.C., 1989. A prediction model for stationary, short-crested waves in shallow water with ambient currents. *Coastal Engineering*, *13*(1), pp.23-54.

Horstman, E.M., Dohmen-Janssen, C.M., Narra, P.M.F., Van den Berg, N.J.F., Siemerink, M. and Hulscher, S.J., 2014. Wave attenuation in mangroves: A quantitative approach to field observations. *Coastal engineering*, *94*, pp.47-62.

Irtem, E., Gedik, N., Kabdasli, M.S. and Yasa, N.E., 2009. Coastal forest effects on tsunami run-up heights. *Ocean Engineering*, *36*(3-4), pp.313-320.

Ishikawa, Y., Sakamoto, T. and Mizuhara, K., 2003. Effect of density of riparian vegetation on effective tractive force. *Journal of Forest Research*, *8*(4), pp.235-246.

Jadhav, R.S., Chen, Q. and Smith, J.M., 2013. Spectral distribution of wave energy dissipation by salt marsh vegetation. *Coastal Engineering*, *77*, pp.99-107.

Järvelä, J., 2002. Flow resistance of flexible and stiff vegetation: a flume study with natural plants. *Journal of hydrology*, *269*(1-2), pp.44-54.

Jordanova, A.A. and James, C.S., 2003. Experimental study of bed load transport through emergent vegetation. *Journal of Hydraulic Engineering*, *129*(6), pp.474-478.

Knutson, P.L., 1977. Planting guidelines for dune creation and stabilization (No. CERC-CETA-77-4). Coastal Engineering Research Center Vicksburg MS.

Knutson, P.L., Brochu, R.A., Seelig, W.N. and Inskeep, M., 1982. Wave damping inspartina alterniflora marshes. *Wetlands*, *2*(1), pp.87-104.

Kobayashi, N., Raichle, A.W. and Asano, T., 1993. Wave attenuation by vegetation. *Journal of waterway, port, coastal, and ocean engineering*, *119*(1), pp.30-48

Koftis, T., Prinos, P. and Stratigaki, V., 2013. Wave damping over artificial Posidonia oceanica meadow: A large-scale experimental study. *Coastal Engineering*, *73*, pp.71-83.

Kothyari, U.C., Tiwari, A.K. and Singh, R., 1997. Estimation of temporal variation of sediment yield from small catchments through the kinematic method. *Journal of hydrology*, *203*(1-4), pp.39-57.

Kothyari, U.C., Hayashi, K. and Hashimoto, H., 2009. Drag coefficient of unsubmerged rigid vegetation stems in open channel flows. *Journal of Hydraulic Research*, *47*(6),

pp.691-699.

Longuet-Higgins, M.S. and Stewart, R.W., 1964, August. Radiation stresses in water waves; a physical discussion, with applications. In *Deep Sea Research and Oceanographic Abstracts* (Vol. 11, No. 4, pp. 529-562). Elsevier.

Løvås, S.M. and Tørum, A., 2001. Effect of the kelp Laminaria hyperborea upon sand dune erosion and water particle velocities. *Coastal Engineering*, *44*(1), pp.37-63.

Ma, G., Kirby, J.T., Su, S.F., Figlus, J. and Shi, F., 2013. Numerical study of turbulence and wave damping induced by vegetation canopies. *Coastal Engineering*, *80*, pp.68-78.

Manca, E., Cáceres, I., Alsina, J.M., Stratigaki, V., Townend, I. and Amos, C.L., 2012. Wave energy and wave-induced flow reduction by full-scale model Posidonia oceanica seagrass. *Continental Shelf Research*, *50*, pp.100-116.

Massel, S.R., Furukawa, K. and Brinkman, R.M., 1999. Surface wave propagation in mangrove forests. *Fluid Dynamics Research*, *24*(4), p.219.

Maza, M., Lara, J.L. and Losada, I.J., 2013. A coupled model of submerged vegetation under oscillatory flow using Navier–Stokes equations. *Coastal Engineering*, *80*, pp.16-34

Mazda, Y., Magi, M., Kogo, M. and Hong, P.N., 1997. Mangroves as a coastal protection from waves in the Tong King delta, Vietnam. *Mangroves and Salt marshes*, *1*(2), pp.127-135.

Mazda, Y., Magi, M., Ikeda, Y., Kurokawa, T. and Asano, T., 2006. Wave reduction in a mangrove forest dominated by Sonneratia sp. *Wetlands Ecology and Management*, *14*(4), pp.365-378.

Mei, C.C., Chan, I.C., Liu, P.L.F., Huang, Z. and Zhang, W., 2011. Long waves through emergent coastal vegetation. *Journal of Fluid Mechanics*, *687*, pp.461-491.

Méndez, F.J., Losada, I.J. and Losada, M.A., 1999. Hydrodynamics induced by wind waves in a vegetation field. *Journal of Geophysical Research: Oceans*, *104*(C8), pp.18383-18396.

Mendez, F.J. and Losada, I.J., 2004. An empirical model to estimate the propagation of random breaking and nonbreaking waves over vegetation fields. *Coastal Engineering*, *51*(2), pp.103-118.

Möller, I., Spencer, T., French, J.R., Leggett, D.J. and Dixon, M., 1999. Wave transformation over salt marshes: a field and numerical modelling study from North Norfolk, England. *Estuarine, Coastal and Shelf Science*, *49*(3), pp.411-426.

Möller, I. and Spencer, T., 2002. Wave dissipation over macro-tidal saltmarshes: Effects

of marsh edge typology and vegetation change. Journal of Coastal Research, 36(sp1), pp.506-521.

Möller, I., 2006. Quantifying saltmarsh vegetation and its effect on wave height dissipation: Results from a UK East coast saltmarsh. *Estuarine, Coastal and Shelf Science*, *69*(3-4), pp.337-351.

Morison, J.R., Johnson, J.W. and Schaaf, S.A., 1950. The force exerted by surface waves on piles. *Journal of Petroleum Technology*, *2*(05), pp.149-154.

Morton, R.A., 2002. Factors controlling storm impacts on coastal barriers and beaches: a preliminary basis for near real-time forecasting. *Journal of Coastal Research*, pp.486-501.

Morton, R.A. and Sallenger Jr, A.H., 2003. Morphological impacts of extreme storms on sandy beaches and barriers. *Journal of Coastal Research*, pp.560-573.

Nederhoff, K., 2014. Modeling the effects of hard structures on dune erosion and overwash; Hindcasting the impact of Hurricane Sandy on New Jersey with XBeach. *Master's thesis Delft University of Technology*.

Paul, M. and Amos, C.L., 2011. Spatial and seasonal variation in wave attenuation over Zostera noltii. *Journal of Geophysical Research: Oceans*, *116*(C8).

Price, W.A., Tomlinson, K.W. and Hunt, J.N., 1969. The effect of artificial seaweed in promoting the build-up of beaches. In *Coastal Engineering 1968* (pp. 570-578).

Quartel, S., Kroon, A., Augustinus, P.G.E.F., Van Santen, P. and Tri, N.H., 2007. Wave attenuation in coastal mangroves in the Red River Delta, Vietnam. *Journal of Asian Earth Sciences*, *29*(4), pp.576-584.

Raubenheimer, B., Guza, R.T. and Elgar, S., 1996. Wave transformation across the inner surf zone. *Journal of Geophysical Research: Oceans*, *101*(C11), pp.25589-25597.

Roelvink, D., Reniers, A., Van Dongeren, A.P., de Vries, J.V.T., McCall, R. and Lescinski, J., 2009. Modelling storm impacts on beaches, dunes and barrier islands. *Coastal engineering*, *56*(11-12), pp.1133-1152.

Roelvink, D., Reniers, A.J.H.M., Van Dongeren, A., Van Thiel de Vries, J., Lescinski, J. and McCall, R., 2010. XBeach model description and manual. *Unesco-IHE Institute for Water Education, Deltares and Delft University of Tecnhology. Report June*, *21*, p.2010

Roelvink, D., McCall, R., Mehvar, S., Nederhoff, K. and Dastgheib, A., 2018. Improving predictions of swash dynamics in XBeach: The role of groupiness and incident-band runup. *Coastal Engineering*, *134*, pp.103-123

Sallenger Jr, A.H., 2000. Storm impact scale for barrier islands. *Journal of Coastal Research*, pp.890-895.

Sánchez-González, J.F., Sánchez-Rojas, V. and Memos, C.D., 2011. Wave attenuation due to Posidonia oceanica meadows. *Journal of Hydraulic Research*, *49*(4), pp.503-514.

Schäffer, Hemming A., Per A. Madsen, and Rolf Deigaard. "A Boussinesq model for waves breaking in shallow water." *Coastal engineering* 20, no. 3-4 (1993): 185-202.

Schambach, L., Grilli, A.R., Grilli, S.T., Hashemi, M.R. and King, J.W., 2018. Assessing the impact of extreme storms on barrier beaches along the Atlantic coastline: Application to the southern Rhode Island coast. *Coastal Engineering*, *133*, pp.26-42.

Schneider, V.R. and Arcement, G.J., 1989. Guide for Selecting Manning's Roughness Coefficients for Natural Channels and Flood Plains. *Available from the US Geological Survey, Books and Open-File Reports Section, Box 25425, Federal Center, Denver, CO 80225-0425. Water-Supply Paper 2339, 1989. 38 p, 22 fig, 4 tab, 23 ref.*

Small, C., Blanpied, T., Kauffman, A., O'Neil, C., Proulx, N., Rajacich, M., Simpson, H., White, J., Spaulding, M.L., Baxter, C.D. and Swanson, J.C., 2016. Assessment of Damage and Adaptation Strategies for Structures and Infrastructure from Storm Surge and Sea Level Rise for a Coastal Community in Rhode Island, United States. *Journal of Marine Science and Engineering*, *4*(4), p.67.

Smith, J.M., Cialone, M.A., Wamsley, T.V. and McAlpin, T.O., 2010. Potential impact of sea level rise on coastal surges in southeast Louisiana. *Ocean Engineering*, *37*(1), pp.37-47.

Smith, J.M., Bryant, M.A. and Wamsley, T.V., 2016. Wetland buffers: numerical modeling of wave dissipation by vegetation. *Earth Surface Processes and Landforms*, *41*(6), pp.847-854.

Smit, P.B., Stelling, G.S., Roelvink, D., van Thiel de Vries, J., McCall, R., van Dongeren, A., Zwinkels, C. and Jacobs, R., 2010. XBeach: Non-hydrostatic model. *Report, Delft University of Technology and Deltares, Delft, The Netherlands*.

Smit, P., Zijlema, M. and Stelling, G., 2013. Depth-induced wave breaking in a non-hydrostatic, near-shore wave model. *Coastal Engineering*, *76*, pp.1-16

Smit, P., Janssen, T., Holthuijsen, L. and Smith, J., 2014. Non-hydrostatic modeling of surf zone wave dynamics. *Coastal Engineering*, *83*, pp.36-48.

Soulsby, R.L. and Whitehouse, R.J.S., 1997. Threshold of sediment motion in coastal environments. In *Pacific Coasts and Ports' 97: Proceedings of the 13th Australasian Coastal and Ocean Engineering Conference and the 6th Australasian Port and Harbour Conference; Volume 1* (p. 145). Centre for Advanced Engineering, University of

Canterbury.

Spaulding, M.L., Grilli, A., Damon, C., Crean, T., Fugate, G., Oakley, B.A. and Stempel, P., 2016. STORMTOOLS: coastal environmental risk index (CERI). *Journal of Marine Science and Engineering*, *4*(3), p.54.

Spaulding, M.L., Grilli, A., Damon, C., Fugate, G., Isaji, T. and Schambach, L., 2017. Application of State of the Art Modeling Techniques to Predict Flooding and Waves for a Coastal Area within a Protected Bay. *Journal of Marine Science and Engineering*, *5*(1), p.14.

Stelling, G. and Zijlema, M., 2003. An accurate and efficient finite-difference algorithm for non-hydrostatic free-surface flow with application to wave propagation. *International Journal for Numerical Methods in Fluids*, *43*(1), pp.1-23.

Stratigaki, V., Manca, E., Prinos, P., Losada, I.J., Lara, J.L., Sclavo, M., Amos, C.L., Cáceres, I. and Sánchez-Arcilla, A., 2011. Large-scale experiments on wave propagation over Posidonia oceanica. *Journal of Hydraulic Research*, *49*(sup1), pp.31-43.

Suzuki, T., Zijlema, M., Burger, B., Meijer, M.C. and Narayan, S., 2012. Wave dissipation by vegetation with layer schematization in SWAN. *Coastal Engineering*, *59*(1), pp.64-71.

Svendsen, I.A., 1984. Mass flux and undertow in a surf zone. *Coastal Engineering*, *8*(4), pp.347-365.

Terrados, J. and Duarte, C.M., 2000. Experimental evidence of reduced particle resuspension within a seagrass (Posidonia oceanica L.) meadow. *Journal of Experimental Marine Biology and Ecology*, *243*(1), pp.45-53.

Thompson, J.R., Sørenson, H.R., Gavin, H. and Refsgaard, A., 2004. Application of the coupled MIKE SHE/MIKE 11 modelling system to a lowland wet grassland in southeast England. *Journal of Hydrology*, *293*(1-4), pp.151-179.

Van Rijn, L.C., 1989. The state of the art in sediment transport modelling. In *Sediment Transport Modeling* (pp. 13-32). ASCE.

Van Rijn, L.C., Walstra, D.J.R., Grasmeijer, B., Sutherland, J., Pan, S. and Sierra, J.P., 2003. The predictability of cross-shore bed evolution of sandy beaches at the time scale of storms and seasons using process-based profile models. *Coastal Engineering*, *47*(3), pp.295-327.

Van Rijn, L.C., 2007. Unified view of sediment transport by currents and waves. I: Initiation of motion, bed roughness, and bed-load transport. *Journal of hydraulic engineering*, *133*(6), pp.649-667.

Van Rooijen, A.A., 2011. Modelling sediment transport in the swash zone.

Van Thiel de Vries, J.S.M., 2009. Dune erosion during storm surges

Vargas-Luna, A., Crosato, A. and Uijttewaal, W.S., 2015. Effects of vegetation on flow and sediment transport: comparative analyses and validation of predicting models. *Earth Surface Processes and Landforms*, *40*(2), pp.157-176.

Vo-Luong, P. and Massel, S., 2008. Energy dissipation in non-uniform mangrove forests of arbitrary depth. *Journal of Marine Systems*, *74*(1-2), pp.603-622.

Wamsley, T.V., Cialone, M.A., Smith, J.M., Ebersole, B.A. and Grzegorzewski, A.S., 2009. Influence of landscape restoration and degradation on storm surge and waves in southern Louisiana. *Natural Hazards*, *51*(1), pp.207-224.

Wamsley, T.V., Cialone, M.A., Smith, J.M., Atkinson, J.H. and Rosati, J.D., 2010. The potential of wetlands in reducing storm surge. Ocean Engineering, 37(1), pp.59-68.

Woodhouse, W.W., 1978. Dune building and stabi-lization with vegetation. Spl. Rep. no. 3. *US Army Corps of Engineers, Fort Belvoir, Virginia*.

Woodruff, J.D., Irish, J.L. and Camargo, S.J., 2013. Coastal flooding by tropical cyclones and sea-level rise. *Nature*, *504*(7478), p.44.

Yusof, K.W., Muhammad, M.M., Mustafa, M.R.U., Zakaria, N.A. and Gahani, A.A., 2017, June. Analysis of Manning's and Drag Coefficients for Flexible Submerged Vegetation. In *IOP Conference Series: Materials Science and Engineering* (Vol. 216, No. 1, p. 012046). IOP Publishing.

Ysebaert, T., Yang, S.L., Zhang, L., He, Q., Bouma, T.J. and Herman, P.M., 2011. Wave attenuation by two contrasting ecosystem engineering salt marsh macrophytes in the intertidal pioneer zone. *Wetlands*, *31*(6), pp.1043-1054.

Zijlema, M. and Stelling, G.S., 2008. Efficient computation of surf zone waves using the nonlinear shallow water equations with non-hydrostatic pressure. *Coastal Engineering*, *55*(10), pp.780-790.

# CHAPTER 2

## "Modeling Damage Levels Associated with Dunes Reinforced with Geotextile Sand-filled Containers (GSCs)"

by

Naser AlNaser[1]; Annette R. Grilli[2]; Stephan T. Grilli[3]; Aaron Bradshaw[4];

Christopher D.P. Baxter[5]; Brian Maggi[6]

Prepared for submission to the Journal of Coastal Engineering

[1] MSc Student, Department of Ocean Engineering, University of Rhode Island, Narragansett, RI 02882. Email: nalnaser.99@gmail.com

[2] Associate Research Professor, Department of Ocean Engineering, University of Rhode Island, Narragansett, RI 02882. Email: annette_grilli@uri.edu

[3] Distinguished Professor and Chair, Department of Ocean Engineering, University of Rhode Island, Narragansett, RI 02882. Email: grilli@uri.edu

[4] Associate Professor, Department of Civil and Environmental Engineering, University of Rhode Island, Kingston, RI 02881. Email: abrads@uri.edu

[5] Professor, Department of Ocean Engineering and Civil and Environmental Engineering, University of Rhode Island, Narragansett, RI 02882. Email: cbaxter@uri.edu

[6] PhD Candidate, Department of Department of Civil and Environmental Engineering, University of Rhode Island, Kingston, RI 02881. Email: bmaggi4@gmail.com

**Abstract**

Permanent application of Geotextile Sand-filled Containers for coastal protection against seasonal storms and hurricanes, lead to the development of new semi empirical hydraulic stability formulas which considers the mechanical properties of the GSC. Assessment tools are required to determine the fragility of a reinforced dune system with GSC during a storm regime. This study presented a numerical model that identifies the damage states associated with these structures. The model combines an existing hydro-morphodynamic software package "XBeach", with two available hydraulic stability equations for GSC. A Hudson's (1956) based stability equation was compared with a more semi-empirical equation proposed by Recio and Oumeraci (2008). Field measurements from a newly constructed project site with dune reinforced with GSCs was used to validate the model against a historical storm that caused damage to the structure. Performance indicators were used to assess the performance of the model and showed excellent morphological and stability predictions of the structure as well as similar predictions of the damage levels observed during TS Hermine

***Keywords**:* Geotextile Sand Containers, dune, XBeach, Surfbeat, soft solutions

## 1. Introduction

Hurricanes and seasonal storms that have increasingly reached and damaged the U.S Atlantic coastline have driven the US federal and state agencies to impose innovative solutions for coastal protection and beach erosion against future events. In a parallel struggle for environmental preservations and habitat restoration, coastal protection measures have evolved to more soft natural based solutions (e.g. Smith et al., 2016). In particular in Rhode Island, the Coastal Resource Management Council (RI CRMC) has

rebuked structural shoreline protection in beaches, dunes, and barrier islands and relies yet on hefty beach and dune nourishment programs.

Over the past decade an increasing number of studies have been addressing coastal hazard and coastal resilience at a global scale (e.g. Baquerizo and Losada, 2008; Vitousek et al., 2017) or more specifically, at regional and local scales. In RI, in particular a series of studies are devoted to assess the risk of coastal communities and barrier islands against extreme storms, sea level rise and climate change (Grilli et al. 2015, 2017a, 2017b, 2017c; Spaudling et al., 2017; Schambach et al., 2018). Results from wave and damage risk models indicated that severe flooding and large damage indexes for residential and commercial structures are expected for the annual 1% of exceedance event (the "100-year" storm). Results of these studies suggest that dune elevation and residential First Furnished Floor elevation (FFFE) are the main factors contributing to reduce the current damage risk of the local coastal communities. Further investigations to evaluate the stability of the dune system during extreme events using a 2-D morphodynamic numerical model has demonstrated the critical importance of a healthy dune and in particular the importance of the vegetation to limit the coastal barrier beaches' erosion and to protect the coastal communities (Schambach et al., 2018).

Although a large number of studies have addressed the question of stability of the GSC when shaped as a protective structure similar to a soft deformable breakwater (e.g. Tekmarine, 1982; Jacobs & Kobayashi, 1983, 1985; Wouters, 1998; Pilarczyk, 2000; Oumeraci et al. 2003; Recio and Oumeraci, 2008; Mori, 2008; Recio and Oumeraci, 2009a, 2009b; Coghlan et al., 2009; Hornsey et al., 2011; Dassanayake and Oumeraci, 2012), there is a large uncertainty on GSC's resilience and efficiency when deploy in-situ.

Indeed, while there is a large number of detailed studies investigating GSC's stability based on numerical modeling with validation from flume/tank experiment, there is a lack of validation of the GSC's deployed in the field, simply because there are very little data available. In addition, the complexity of the structures shaped as breakwaters but formed of deformable elements, each behaving differently according to its position in the structure and the specific of the environmental forcing (e.g. up-rush, down-rush) led recent studies to question the applicability of the fundamental equations used for the design (Recio and Oumeraci 2008, 2009a, 2009b, Dassanayake and Oumeraci 2012, 2013).

The potential use in Rhode Island of GSCs structures as dune reinforcement to protect vulnerable structures against austere environment is currently being considered. Post-construction surveys have been undertaken to assess and validate available design codes and to assess the structure performance under future storms. In order to optimize the future design of the GSC's structure in RI as well as to predict its behavior and resilience in the current wave climate, including extreme storms, as well as in the predicted close future climate (25 years), we propose to study the GSCs' behavior recently deployed southerly from RI on the New England shoreline, in Montauk, NY. We propose to model the environmental forcing and verify the state-of –the art hydraulic stability's formulations originally derived from in-situ's experiments (Dassanayake and Oumeraci, 2012). We use the 2-D hydro-morphodynamic model XBeach (Roelvink et al. 2009, 2010, 2018) to simulate recent storms and their associated erosion at the Montauk GSC's site. Field data were indeed collected at the site for the recent Tropical storm Hermine (Septemner 2016) 6 months after completion of the GSC's structure. The main

steps of the study are:

[1] Validation of XBeach using Tropical storm Hermine to simulate the erosion at the site.

[2] Validation of Oumeraci's team stability equations.

[3] Development of Numerical model that predicts the damage level of a dune structure reinforced with GSCs.

While the present approach is deterministic, in a phase 2, we address the damage assessment in a stochastic approach providing fragility curves for the structure as deployed at the site. A description of the site is presented in Section 2; in Section 3, we describe the methodology. Input data required for model and equations are described in Section 4. Results are provided in Section 5, followed by discussion and conclusion in Section 6 and 7 respectively.

**2. Site Description**

The increase in storm frequency combined with the urbanization of the dune prevents the natural restoration of beach systems and limit their role of protective buffer zones along the sandy coastlines of Long Island, resulting in an increasingly higher risk imposed on coastal developments and insurance agencies (Woodruff et al., 2013; Blake et al., 2013). To improve coastal resiliency of the downtown area of Montauk, NY and to minimize the risk sustained by coastal front developments, the USACE has built a dune system reinforced with GSCs. The objective of the new synthetic dune system is to limit the beach erosion and protect the dense community settled at the top of the dune barrier. Completed in March 2016 at a total cost of $10 million, it remains the only funded federal project of its type. A further description of the site and some photographs of

structural damages caused by hurricane Sandy 2012 are presented in Figure 2.1.

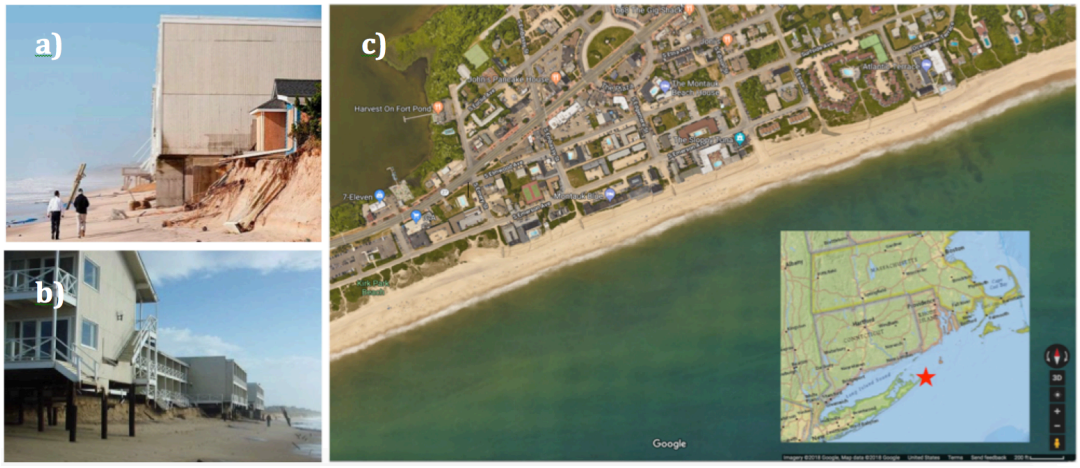


***Figure 2.1*** *Description of the project site. a) and b) Photographs taken after Hurricane Sandy 2012 of coastal front structures. c) Aerial photographs of downtown Montauk, NY taken from Google maps after completions of the project.*

The 800m stretch of the GSC structure expands at the top of the beach parallel to the line of coastal front development. The project consumed 11,000 non-woven GSCs of typical dimensions (1.67x0.9x0.3m) using 109,000 cubic yards of sand with similar characteristics to that found in site for 80% filling ratio. GSCs were placed longitudinally using two armor layers at a slope of 1:2. The structure is 3 meter high and has a crest elevation of 3.8m NAVD88. The design of the structure is shown in Figure 2.2. As-Built elevation surveys were undertaken for a number of transects along the project (USACE-NAN, 2014).

Post construction surveys recorded several consecutive storms that hit the project. Tropical Storm (TS) Hermine (September 2016) hit the site 6 months after completion followed by a Nor'easter 4 months after. These storms generated high waves with offshore significant wave heights of 4 and 6 m respectively (NOAA), causing severe erosion of the beach's berm and exposure of the GSC layer. Post analysis of the site revealed that the cyclonic nature of storms causes erosion in the east side of the site and

deposition on the west side. The middle region is considered to be the most sensitive for the local economy with 3 major hotels located in this area. Post survey photographs are shown in Figure 2.3 for this region.

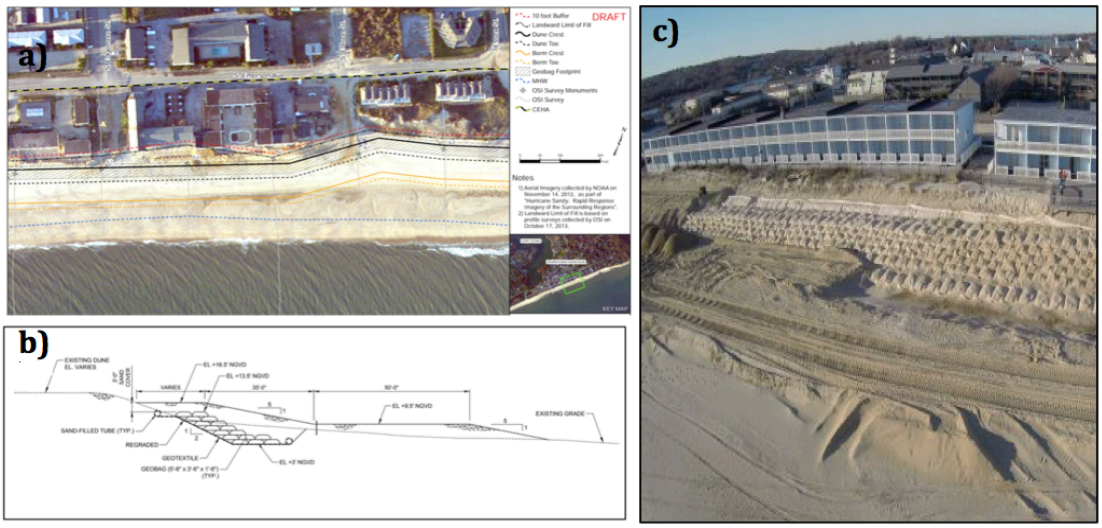


***Figure 2.2*** *Project Details. a) and b) Typical plan and cross section of the As-built drawings respectively (USACE-NAN, 2014). c) Aerial photography taken during construction of the project (Photo credit by TenCate).*


**Figure 2.3** Post construction surveys and monitoring. *a) Photo taken in September 6, 2016 during TS Hermine. b) Photo taken in September 9, 2016 after TS Hermine. c) Photo taken during January 24, 2017 Nor'easter storm. (Photo credit: Brian Maggi)*

## 3. Methodology

In this study we investigate the adequacy of available hydraulic stability equations for predicting damage levels for reinforced dunes with GSCs in barrier beaches during a storm regime. Field survey performed after TS Hermine provide data to validate the models used in the study. A brief description of formulations and models used is presented in this section. While this study is part of a larger research project seeking to develop fragility curves for the GSC based on a stochastic approach of the hazard, the objectives of this component of the project are:

[1] Validate XBeach to predict the dune erosion at the GSC site using field survey performed after TS Hermine damaged the site.

[2] Investigate the adequacy of state of the art's stability equations for predicting damage level on reinforced dunes with GSCs (Oumeraci, 2012) by comparing with field observations.

[3] Assess if these models and approaches are adequate to be used for phase 2, which is developing a fragility curve to estimate the damage levels associate with reinforced dunes with GSCs.

### *3.1 Damage levels of Reinforced Dune with GSCs*

Damage levels refer to Dassanayake and Oumeraci's classifications (2013) in which damages are classified into two sub-classification, I classification 1, damages are identified at the scale of a single GSC, while in classification 2 damages are identified at the scale of the entire GSC's structure. Some authors (Shirlal and Mallidi, 2015) summarized the results in a level 3 classification, where the total fraction of the damage structure is estimated as the percentage of GSCs displaced with respect to total GSCs in

the structure. We introduce a level 4 classification where the full beach is considered and the erosion on the entire ecosystem beach and GSC's structure is considered (Table 2.1).

*Table 2.1 – Damage levels for Reinforced Dune with GSCs*

| Damage Level | Description | Associated Risk |
|---|---|---|
| 0 | Accretion or no change of the profile | No Risks |
| 1 | Erosion of the berm | Replenishment costs |
| 2 | Erosion of GSCs cover layer or the dune | Replenishment costs |
| 3 | Exposure of GSCs | Replenishment costs |
| 4 | Hydraulic instability of GSCs | Structure failure and instability |
| 5 | 0.5m Scour Development | Structure failure and instability |
| 6 | Wave run up exceeding crest elevation, overtopping, and submergence of structure | Flooding and damage to coastal front developments |

*3.2 Hydro-morphodynamic Model XBeach*

The XBeach ("eXtreme Beach behavior") software package was selected to quantify damage levels 0,1,2,3,4 and 6, as well as required hydrodynamic conditions to calculate hydraulic instabilities of GSCs for damage level 5. XBeach is a 2-D coupled hydrodynamic and morphodynamic model that dynamically simulates the coastal response during time-varying storm conditions, and consequently the storm-induced changes in bed level (Roelvink et al., 2009, 2010). The model is designed to simulate processes occurring during the four erosion regimes defined by Sallenger (2000), swash, collision, overwash and inundation, on coarse-grained beaches, dunes and barrier islands. The key advantage of using XBeach for this study is its algorithm for calculating dune avalanching and ability to resolve long waves and ultimately the swash motions that dominate the sediment transport at the foreface of the dune. Furthermore, it offers a choice of hydrodynamic models and sediment transport models combined to a

morphology change model. Wave and sediment transport modules selected for this study are briefly described.

*3.2.1 Wave Propagation and Transformation Module*

The "Surfbeat" model was selected which simulates mean currents in combination with a wave action conservation equation. The characteristic feature of this model is the modeling of the long wave component of swash motions, the surf-beats resulting from the forcing by wave groups of infragravity waves and causing slow oscillations of the mean water level directly related to foreshore erosion (Longuet-Higgins and Stewart, 1964; Van Rooijen, 2011). Surf-beats are indeed particularly dominant in the surf zone in storm conditions, since the high frequency band is saturated, while the low infra-gravity frequency band is not, particularly on dissipative beaches (Raubenheimer and Guza, 1996). While the full directional distribution of wave action is maintained, the frequency spectrum is limited to a single frequency, the peak frequency. The propagation of wind waves is based on the conservation of wave action equation, coupled to a roller energy balance equation (Svendsen, 1984) in the surf zone through the wave dissipation term. Radiation stress tensors acting as forcing terms for depth- and period-averaged mean current equations are expressed based on linear wave theory. The mean current equations are the standard 2D nonlinear shallow water equations expressed in a Generalized Lagrangian Mean (GLM) formulation. Bottom shear stress terms are estimated based on the Eulerian velocity occurring at the seabed using friction coefficients. The 2D depth-averaged equations are used to model the infragravity waves.

Although non-linear properties of short waves which are not represented by linear wave theories, such as asymmetry, skewness and turbulence and are only parameterized;

the surf-beat approach has been validated on dissipative beaches with a surf similarity parameter ranging from 0 – 0.55 (mild conditions) (e.g. Nederhoff, 2014; Schambach et al. 2018; Van Rooijen et al. 2011; De Vet et al., 2015). Indeed on dissipative beaches the short waves are mostly dissipated by the time they reach the shoreline, and only infra-gravity reach the shoreline.

*3.2.2 Sediment Transport Module*

The sediment transport model used in this study is the default model in XBeach introduced by Van Rijin (2007) and further developed by Van Thiel (2009). It is based on the depth-averaged advection-diffusion equation proposed by Galappattiand and Vreugdenhil (1985). The sediment transport is controlled by the sediment concentration in the water column relative to an equilibrium concentration (Soulsby, 1997). While wave propagation equations are based on linear theory, the effect of non-linear waves on sediment transport is included by adding an arbitrary parameterized advection velocity $u_a$ (Stokes drift) to the Eulerian velocity, based on a wave skewness $S_k$ and asymmetry $A_s$, both weighted by arbitrary coefficient, $f_s$ and $f_a$ (facua parameter) (Roelvink et al., 2010). Higher facua value will result in more nonlinearity of the wave shape and hence more landward sediment transport.

*3.2.3 Model Parameters*

Default model parameters were used, except for those where extensive set of validation and recommendations were provided through comparative field analysis and laboratory experiments (Nederhoff, 2014; Devet et al., 2015; Van Rooijen, 2011; Roelvink, 2009; Elsayed and Oumeraci, 2017; Schambach et al., 2018). Such parameters are bed friction coefficients, wave skewness and Assymetry “facua” parameter,

morphodynamic accelerator factor “morfac”, critical wet and dry slope avalanching value, and scaling factor “eps”.

[Note that we used XBeach version Kingsday v1.22.4867), released with the netcdf and MPI options.]

*3.3 Hydraulic stability equations*

While early GSC-structures were designed using the hydraulic stability formula for rubble mound armor layers such as Hudson’s formula (1956), this formulations were not appropriate for deformable structures in marine environment and were progressively replaced with new semi-empirical formulations based on tank/flume experiments using specific GSC arranged in selected structural shape within a controlled wave environment.

Wouters (1998) using experimental data (Bouyze and Schram, 1990), developed Hudson’s equation to account for wave period and steepness using the surf similarity parameter, as well as using different characteristic length to account for geometric variation of the structure’s elements. Using Wouters’ formula (1998) Oumeraci (2003), proposed new stability criteria for GSC’s placed either on the slope or on the crest of the structure, expressed as:

$$N_{s,slope} = \frac{H_s}{\left(\frac{\rho_E}{\rho_w} - 1\right) \cdot D} < \frac{2.75}{\sqrt{\xi_0}} \quad (2.1)$$

$$N_{s,crest} = \frac{H_s}{\left(\frac{\rho_E}{\rho_w} - 1\right) \cdot D} < 0.79 + 0.09\frac{R_c}{H_s} \quad (2.2)$$

where $N_s$ is the stability number of the element, $H_s$ is the significant wave height at the toe of the structure, $\rho_E = (1 - n) \cdot \rho_s + \rho_w \cdot n$ is density of the GSC element , $\rho_w$ and $\rho_s$ is

the density of water and sand respectively, $D = l \cdot sin\alpha$ is the thickness of the first armor layer, $l$ is the length of the GSC, α is the structure slope, $\xi_0 = tan\alpha / \sqrt{\frac{H_0}{L_o}}$ is the surf similarity parameter, function of the slope and deep water wave characteristics, $L_O$ and $H_O$, the deep water significant wave height the wavelength respectively.

More recent studies, questioning the applicability of Hudson's hydraulic stability formulation for GSC structures, provided new formulation to assess the stability of the GSCs (Recio and Oumeraci, 2008; Dassanayake and Oumeraci, 2012). Indeed, GSCs, unlike rock armors are deformable, and do not behave as rigid elements, showing different mechanical properties under cyclic loading, as permeability, flexibility, and sand-fill ratio. A stress-strain analysis revealed that the increase of the GSC effective area during uprush, contribute to larger forces and moments acting on the GSC than during downrush and that a steeper slope of the structure would increase its stability. Numerical simulations for a number of structure configurations, validated with tank experiments, led to empirical relationship relating flow velocity and acceleration, deformation factors for drag, lift, resisting, and advection forces, geometrical characteristics (length) and locations of the GSC (i.e. slope or crest). Recio and Oumeraci (2008) provided the first "process-based" stability equations for GSCs. Such equations are presented hereafter for two failure modes, sliding and overturning:

$$l_{c(sliding)} < u^2 \frac{[0.5KS_{CD}C_D + 2.5KS_{CL}C_L\mu]}{[\mu KS_R\Delta g - KS_{CM}C_M \frac{\partial u}{\partial t}]} \quad (2.3)$$

$$l_{c(overturning)} < u^2 \frac{[0.05KO_{CD}C_D + 1.25KO_{CL}C_L]}{[0.5KO_R\Delta g - 0.1KO_{CM}C_M \frac{\partial u}{\partial t}]} \quad (2.4)$$

where $l_c$ is the length of the container, u is the horizontal flow velocity. $KS_{CD}$, $KS_{CL}$, $KS_R$, $KS_{CM}$ are deformation factors for drag, lift, resisting, and advection forces respectively. Similarly $C_D$, $C_L$, $C_M$ are coefficients for drag, lift, and advection respectively. μ is the viscosity of water, and g is gravitational acceleration.

*3.4 Assessment and Evaluation Methods*

The ability of the model to simulate accurately the eroded volume is assessed applying several skill parameters. A summary of the skill parameters of the model used to assess the accuracy of the model for each scenario is presented in Table 2.2. Parameters are the Brier (BSS) and Bias (BI) scores, the Root Mean Square Error (RMSE), and the skill of the model as defined by Gallager et al (1998) (SKG), and used in Schambach et al. (2018) that compares the relative value of the eroded volume.

*Table 2.2 – Summary of skill parameters used to assess the Simulation Results*

| Statistical Skill Parameter | Conceptual assessment | Optimal value | Formulation |
|---|---|---|---|
| SK | Relative value of the eroded volume | 1 | $SK = 1 - \frac{\sqrt{\sum_{i=1}^{N}(V_c - V_o)^2}}{\sqrt{\sum_{i=1}^{N} {V_o}^2}}$ |
| BSS | Morphological skill to compute bed level change | 1 | $BSS = 1 - \frac{\sum_{i=1}^{N}\left(z_{b,comp} - z_{b,meas}\right)^2}{\sum_{i=1}^{N}\left(z_{b,initial} - z_{b,meas}\right)^2}$ |
| BI | Difference in central tendencies of computed and observation | 0 | $BI = \frac{1}{N}\sum_{i=1}^{N}\left(z_{b,comp} - z_{b,meas}\right)$ |
| RMSE | Accuracy of computed results | 0 | $RMSE = \sqrt{\frac{1}{N}\sum_{i=1}^{N}\left(z_{b,comp} - z_{b,meas}\right)^2}$ |

## 4. Data and Model Setup

Bathymetric, topographic and hydrodynamic data were needed to simulate TS Hermine, the first storm to hit the project 6 month after completion. These were obtained from various sources; and processed as input data for our 2-D numerical model XBeach. Further description of required input data and model set up can be found in their manual (XBeach Manual). This section only gives a brief description of our model set up and data used.

### *4.1 Topographic Data*

Pre topographic conditions for the TS Hermine simulation used several data sources. As-Built drawings and survey measurements provided by the USACE were used to construct the backshore of the beach and the cover layer of the GSCs. These measurements were taken at number of transects along the project site using real-time kinematic global positioning system (RTK-GPS), and were provided in State Plane horizontal coordinate system, and NAVD88 as vertical plane coordinate system both in metric system. Elevations of the dune area up to the landward end of the model domain were obtained from LiDAR survey measurements taken in October 31, 2017 procured by the USACE at very high resolution (less than 1x1m) (USACE, Personal Communication, 2016). These areas were not inundated by storm surge since the completion of the project and can well represent the pre-storm conditions. Further interpolation and smoothing of the data were undertaken for the two different sources to generate a 0.5x1.2m grid of the model near the project site. In addition, the LiDAR survey measurements include the elevation of building structures located behind the dunes. These locations were filtered out from the survey and used in the simulation to assess their vulnerability against

damage level 6.

Post survey measurements of TS Hermine were used to validate XBeach results. These were taken on September 9, 2016 one day after the storm has dissipated. Using RTK-GPS, 22 transects along the project were measured. These are also provided in similar coordinate systems to pre survey measurements. Figure 2.4 shows a 2-D plot of the data sources used to construct the topography of the model and transect locations for both as-built and post surveys measurements. It can be clearly seen that the dunes on the west and east side of the area are located behind the coastal front of 3 major hotels, leaving them vulnerable to wave attacks.

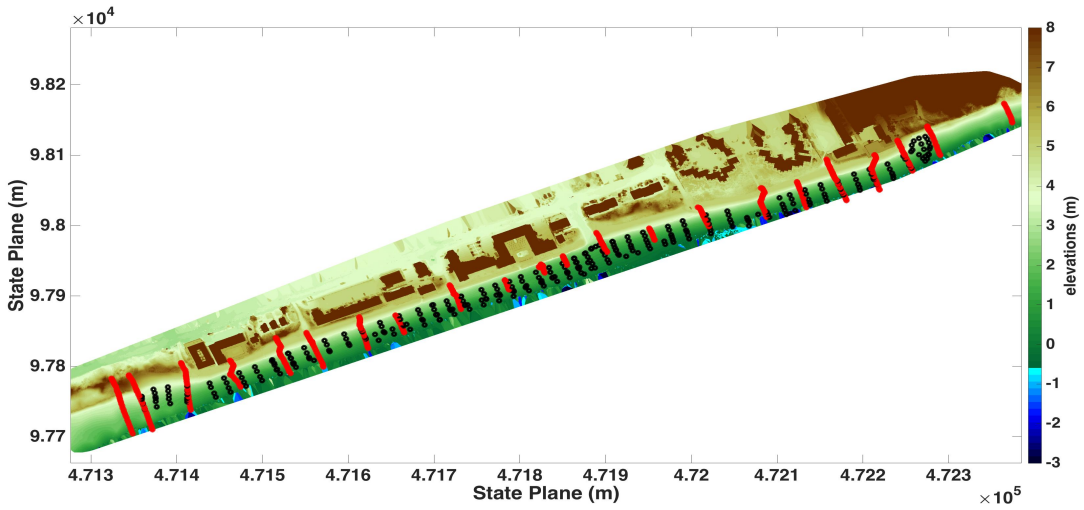


***Figure 2.4*** *Topographic data sources used to simulate TS Hermine. Black dots indicate As-Built survey measurements taken in June 2016 after completion of the project. Red dots refer to post survey measurements of TS Hermine.*

*4.2 Geotextile Sand-filled Containers (GSCs)*

The GSCs' locations were required to specify them as a *non-erodible* layer in XBeach. They were also specified as save points to output velocities and significant wave heights and to ultimately determine the hydraulic stability of the GSCs (Equations 2.1 – 2.4). Figure 2.5 shows an example of a cross section of the constructed model, including

location of GSCs layer.

***Figure 2.5*** *A cross sectional example of the location of the GSCs layer as constructed in the model treated as non-erodible layer in XBeach. The black line indicates the bed level, and blue line refers to the GSCs layer*

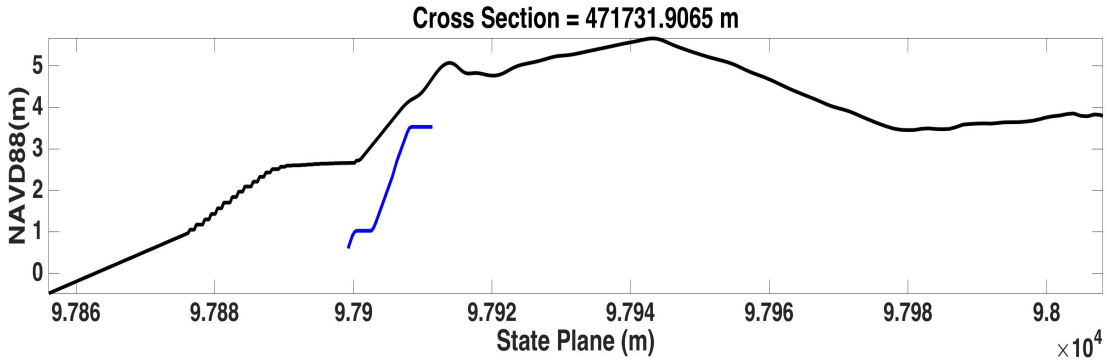


*4.3 Computational grid and Model Setup*

To have a full XBeach model domain, bathymetric data was combined with the topographic data described in section 4.1. These were obtained from National Ocean and Atmospheric Agency (NOAA) Digital Coast database available on their website; and covers the full area domain. The resolution of the data is 1x1m. This was further interpolated to 5x1.2m offshore and 2x1.2 near-shore. The bathymetric data was published in 2015, and therefor some differences in the bed level at the interface of each data set (topo vs. bathy) was observed when combining the data. In addition several offshore bars were observed in the data and were removed to avoid un necessary dissipation of the incident waves.

The computational grid used the final topo-bathy rotated 22 degrees clockwise about its offshore origin from the east direction to have the shoreline parallel to the axis line as required by the model. In addition to the GSCs layer, building elevations and locations were included as non-erodible layer, to simulate long and short wave run-ups, long wave

reflection, scouring (Figure 2.6).

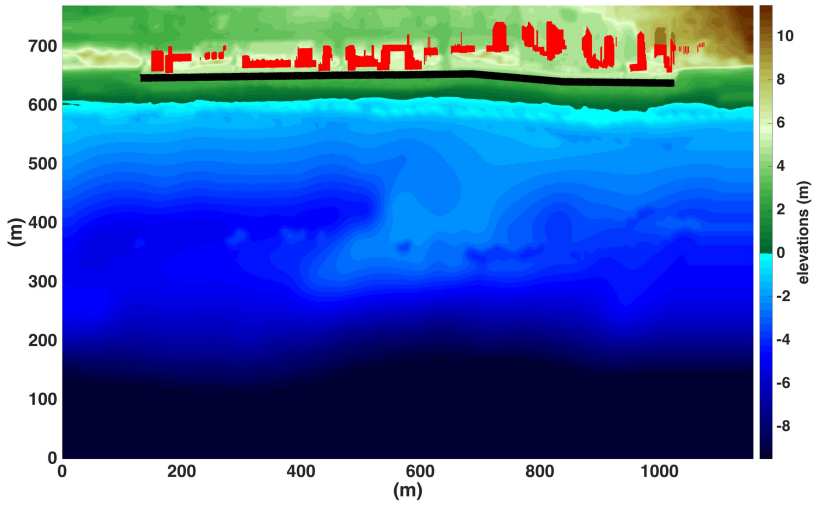


***Figure 2.6*** *Final XBEACH model set up. Combined topo-bathy and non-erodible layers at a rotated grid 22 degree clockwise from the offshore origin. Black and red shading indicates non-erodible locations for GSCs and building structures respectively.*

*4.4 Hydrodynamic Boundary Conditions*

Hydrodynamic Boundary conditions at the offshore location of our computational grid for TS Hermine were specified. Time series of water levels were obtained from NOAA tidal buoy 8510560, Montauk NY, reasonably close to the site (Figure 2.7). Wave measurements however, were only available far offshore at NOAA's wave buoys 44017 (Figure 2.8). Consequently waves were propagated from the buoy's location to the offshore boundary of the XBeach coastal computational grid using Steady State Spectral Wave model (STWAVE). STWAVE is a 2-D numerical wave model based on the wave action balance equation, assuming stationary waves (i.e. $\partial E/\partial t=0$) (Smith et al. 2001).

Energy density spectrums were obtained from NOAA's wave buoy in 1D. A directional spreading function based on Mitsuyasu-type (Mitsuyasu et al. 1975) was applied to generate a 2-D wave spectrum used in input to simulate the wave propagation using STWAVE. For this larger scale wave propagation we used NOAA's topographic

and bathymetric data (NOAA National Center for Environmental Information) at 9 m resolution. STWAVE was run on a 60 m grid shown in Figure 2.8.

TS Hermine's simulation time was 96 hours, starting September 4, 2016 00:00:00 UTC During this period,, the storm track was relatively close to the project site to generate waves characterized by a significant wave heights greater than 1m. The peak of the storm occurred around September 6, 2016 00:00:00 UTC (49 hours after start of the simulations) with offshore significant wave heights of the order of 4.5m, peak period of 11s, and maximum surge of 0.8m NAVD88 (Figure 2.9).

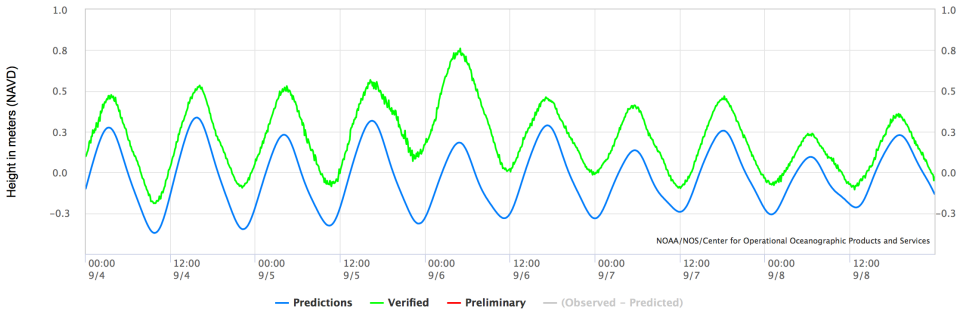


***Figure 2.7*** *Water level measurements during TS Hermine taken at NOAA's buoy 8510560 close to the site location.*

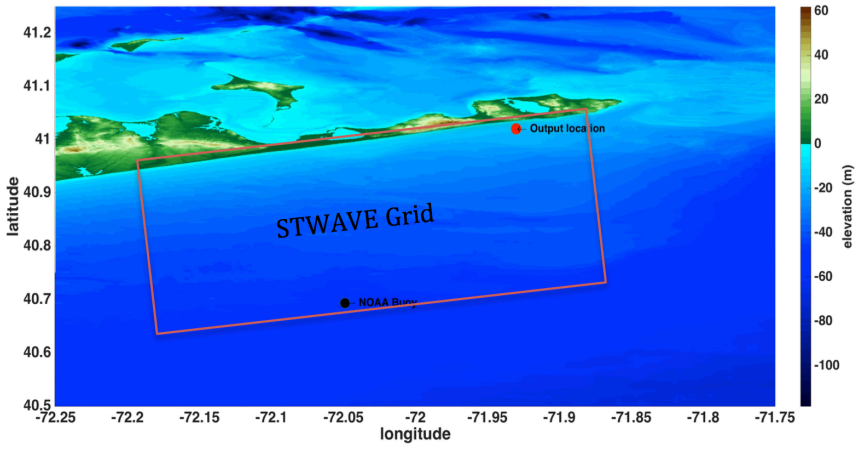


***Figure 2.8*** *STWAVE model domain rotated at 22 degrees counterclockwise. Black dot indicating location of wave measurements taken from NOAA's buoy. Red dot indicates time series of wave heights output location as XBeach boundary conditions.*

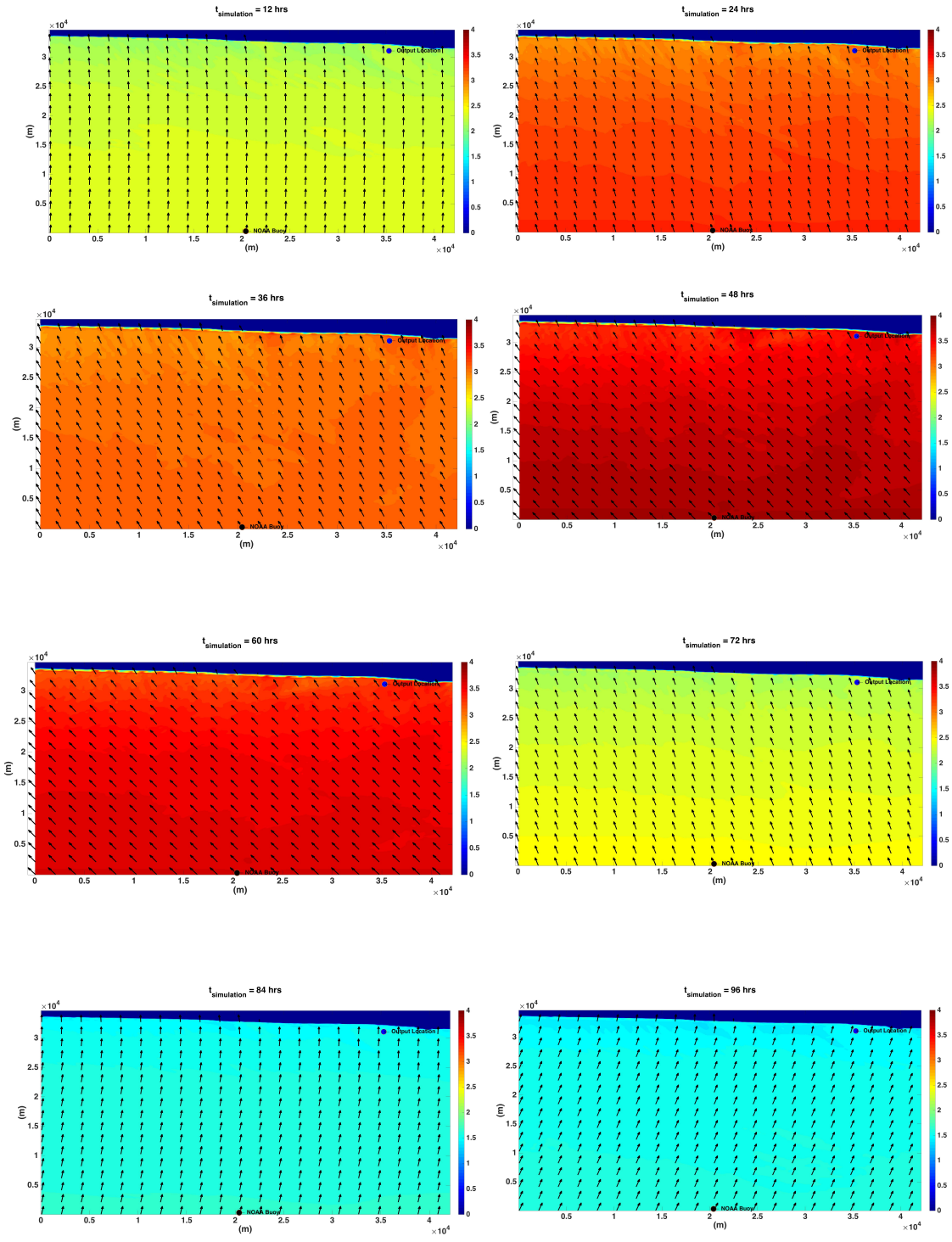


**Figure 2.9** *Time steps of TS Hermine in STWAVE simulation. Black dot indicating location of wave measurements taken from NOAA's buoy. blue dot indicates time series of wave heights output location as XBeach boundary conditions.*

Due to the uncertainty in the data for both (1) STWAVE Results due to the large discretization of the computational grid which is expected to result in lower peak wave heights, as well as the (2) bathymetric conditions used for the XBeach computational grid; certain adjustments to the hydrodynamic boundary conditions were made to account for these uncertainties and to obtain an upper confident level of the results. Especially when XBeach is shown to be very sensitive to the significant wave heights (Nederhoff, 2014) and water depths. Any under specification of the offshore wave conditions might lead to lower estimation of erosion. Therefore to ensure the development of Damage level 3 (exposure of the bag) and validate the hydraulic stability equations (Section 3.3) for predicting Damage level 4, the significant wave heights at the offshore boundary were increased by 25%. In addition, the water levels obtained from the NOAA offshore Buoy were increased by 10% to account for uncertainty in the near shore bathymetry which may lead to additional dissipation of the incident waves.

## 5. Results

First, results of predicted bed level changes are compared with post survey measurements using standard morphological skill parameters. Then, predicted damage levels (Section 3.1) are assessed using both Oumeraci (2003) and Recio and Oumeraci ‘s stability formula (2008).

### *5.1 TS Hermine Bed Level Changes*

Bed level change analysis of the XBeach results indicated intense erosion of the berm as well as the cover layer of the GSCs. Since TS Hermine hit the coastline in collision regime, avalanching was the principal process responsible for the beach morphological changes resulting in cover layer and berm’s erosion and offshore sediment

transport, with rapid deposition in the beach backshore (Figure 2.10). Erosion and deposition shows a relatively homogeneous behavior along the entire beach section.

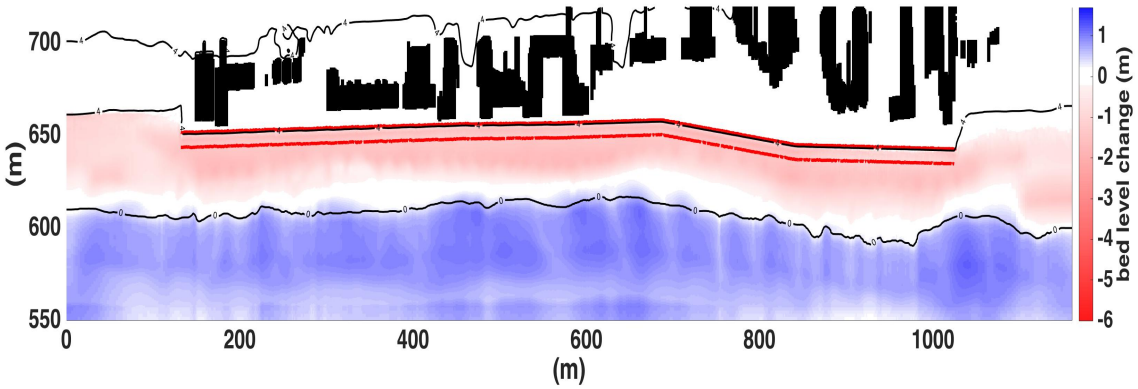


***Figure 2.10*** *Calculated bed level change for TS Hermine. Red line indicates the location of the GSC structure. Black shading refers to the location of buildings. Contour lines are shown for 0m and 4m.*

A detail comparison of measured and simulated erosion shows a spatial variability in observed eroded volume along the beach, reproduced with variable accuracy by simulations (Figure 2.11). Indeed measurements show an asymmetry in the sediment erosion/acretion pattern associated to a slight asymmetry in the coastal topography (east side is relatively higher) and to a likely longshore current, resulting in larger sediment accretion at the west side of the site. The middle area (in front the 3 major hotels) shows the most intense erosion of the berm, causing exposure of the GSC layer. Although numerical simulations do not reproduce the details of this observed asymmetric pattern, they capture relatively closely the erosion observed in the middle region where exposure of the GSC occurred (red line in Fig. 2.11).

The beach is schematized in 3 sub-zones characterized by their general pattern in erosion/accretion as well as model's performance (Figure 2.12). Zone A, the west side of

the site where accretion was observed but however not predicted; indeed the model predicts exposure of the bag. Zone B, the middle region where GSC's exposure is observed, as well as predicted. Zone C, eastern side of the beach where only the erosion of the berm was observed and predicted.

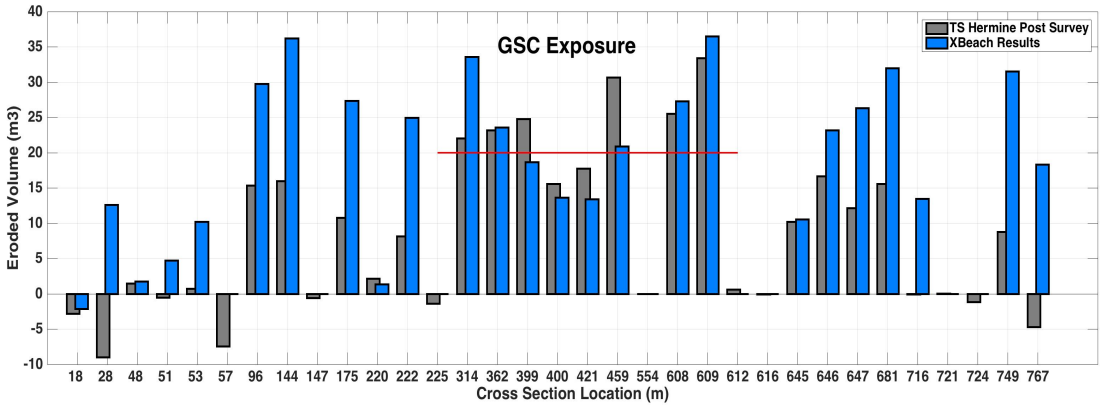


***Figure 2.11*** *Comparison between the measured and calculated Eroded volume from XBeach at each transect profile along the length of the structure. Red line indicates location of GSC exposure; negative values indicate accretion.*

The model's performance is assessed for each zone based on standard model's skill parameters averaged for each morphological sub-zone (Section 3.4). Results are summarized in Table 2.3. Zone A show a "poor" performance. Indeed the predicted morphological response is inaccurate with large errors and low skill score; An "Excellent" performance is obtained in Zone B, with an average of the Brier Skill Score (BSS= 0.83), indicating good morphological predictions. Eroded volume was accurately calculated resulting in a high Gallegher Skill Score (SK=0.63) and low Bias Score (BI=0.18 m). A Reasonable performance is achieved in Zone C, predicting correctly the non-exposure of the GSCs, although the eroded volume is over estimated, leading to low scores. Typical cross section profiles of the bed level change for each zone is provided in

Figure 2.13, to further illustrate the performance of the model.

*Table 2.3 – Summary of Performance Evaluation Assessment for Each Zone*

| | | |
|---|---|---|
| **Zone A (Area with Deposition)** | **Brier Skill Score (BSS)** | -13.03 |
| | **Bias Score (BI)** | -0.41m |
| | **Root Mean Square (RMS)Error** | 0.69m |
| | **Gallegher Skill Score (SK)** | 0.26 |
| **Zone B (GSC Exposure Area)** | **Brier Skill Score (BSS)** | 0.83 |
| | **Bias Score (BI)** | 0.18m |
| | **Root Mean Square (RMS)Error** | 0.46m |
| | **Gallegher Skill Score (SK)** | 0.67 |
| **Zone C (Eroded Area but without Exposure)** | **Brier Skill Score (BSS)** | -3.25 |
| | **Bias Score (BI)** | -0.27m |
| | **Root Mean Square (RMS)Error** | 0.46m |
| | **Gallegher Skill Score (SK)** | 0.30 |

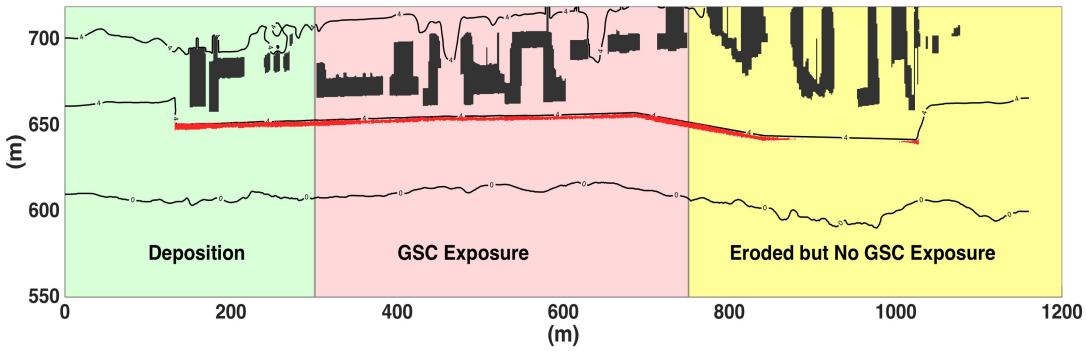


***Figure 2.12*** *Sub-categorization of the site. Red shading indicates exposed location from XBeach simulation. Grey shading referes to building locations. Contour lines are shown for 0m and 4m.*

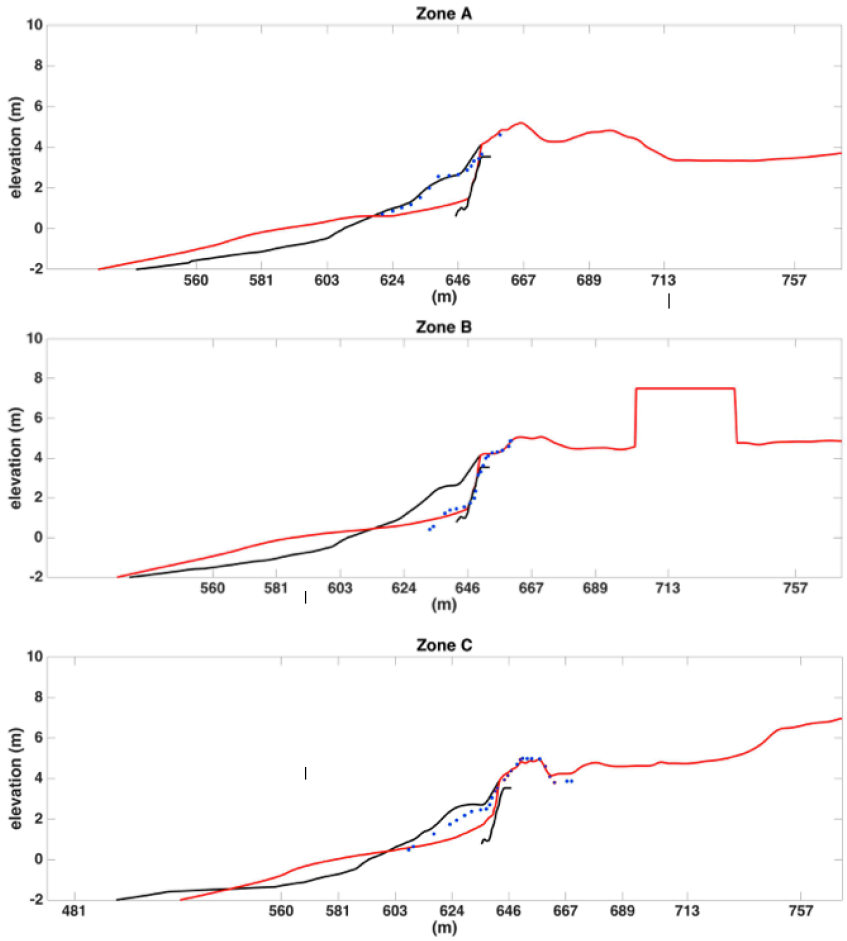


***Figure 2.13*** *Typical Cross sectional profiles of the bed level change for each zones. Blue dots refer to post measurements. Black indicates the initial bed level, and red line refers to XBeach Results. The location of the GSC structure is also shown with black.*

*5.2 TS Hermine Damage Levels*

Results of the simulations are used to predict damage levels (Table 2.1 at each location of the GSCs' structure. Bed level changes are used to determine damage level 0-3. For GSCs' exposed locations hydraulic stability equations (Section 3.2) are applied to determine if damage level 4 is likely to occur. Damage level 5, is only calculated for GSCs located along the structure's toe. Maximum water levels are used to determine if damage level 6 is likely to occur. Figure 2.14 provides the estimated damage levels based on Oumeraci (2003) and Recio and Oumeraci (2008)'s hydraulic stability equations.

Hudson's based stability formula proposed by Oumeraci 2003, did not give any predictions of GSC instability along the entire length of the structure. Recio and Omeraci (2008)'s stability equation, predicts 1 instable GSC occurring during peak conditions. Although 1 displaced GSC was also observed during survey measurement (Figure 2.3), the location of the predicted displaced bag is not accurately predicted. Furthermore Damage 5 and 6 did not occur during TS Hermine, and was therefore not predicted by the model.

*5.3 Hydraulic Stability of GSCs*

Stability equations (both formulations, Oumeraci (2003) and Recio and Oumeraci (2008)) are used at each exposed location to assess the GSCs' stability and the performance of the structure, providing a quantitative method to identify vulnerable locations. The Hudson's based stability equation (Oumeraci, 2003) suggests that all of exposed locations were still in stable conditions during the storm. Figure 2.15a plots the maximum calculated stability number at each location during the storm. It can be seen that these remained well under critical conditions. This however was not suggested by

Recio and Oumeraci (2008) formula, in which 3 locations were identified to be vulnerable during the storm. Two of these locations are located in Zone B, which is the most sensitive region. Figure 2.15b shows the suggested minimum required GSC's length to prevent displacement of each of the exposed GSCs. Except for 1 location, all the GSCs showed to have sufficient length to prevent displacement.

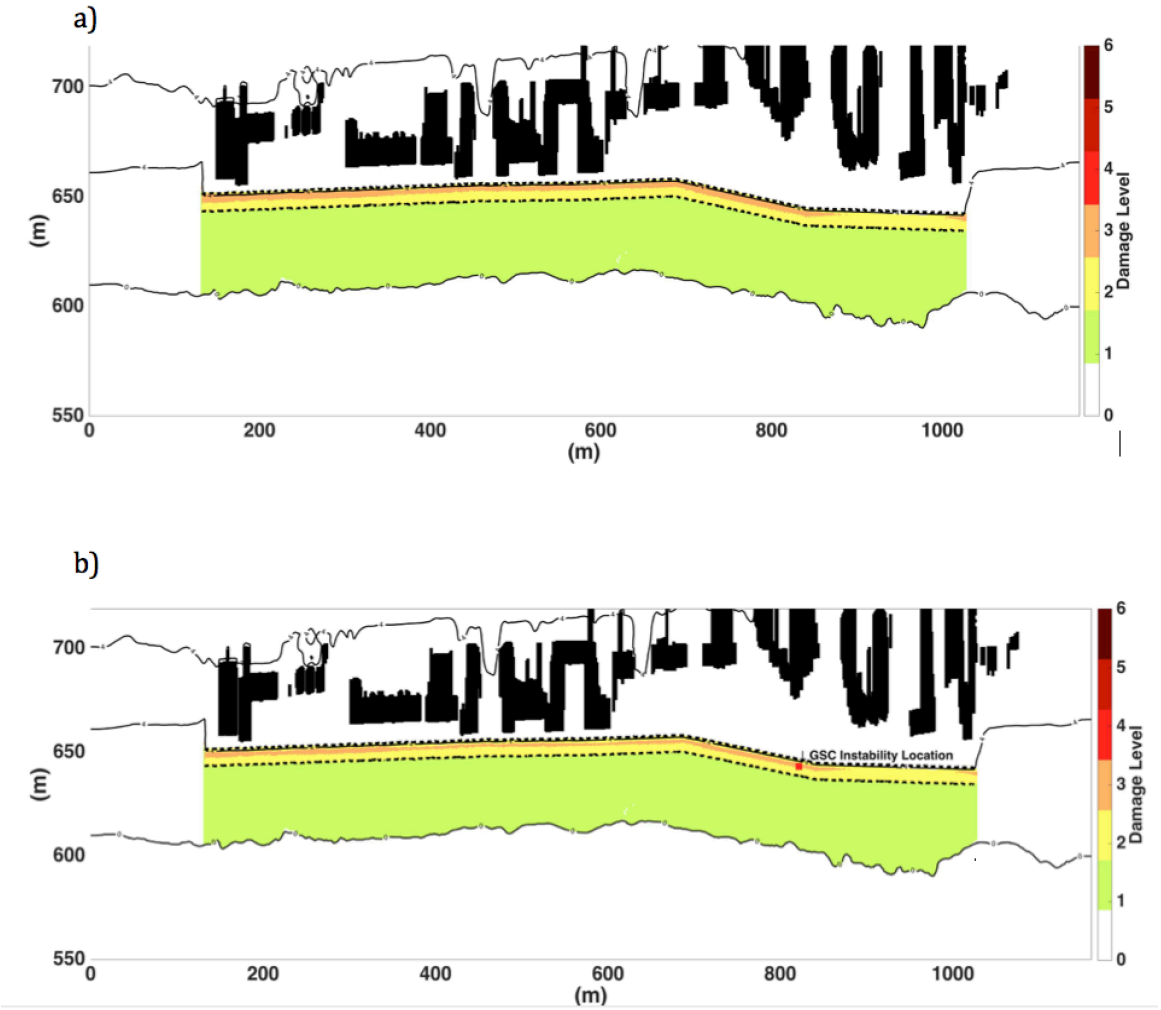


***Figure 2.14*** *Calculated Damage levels for TS Hermine, using a) Omeraci 2003 and b) Recio and Omeraci 2007 hydraulic stability formula for GSCs.*

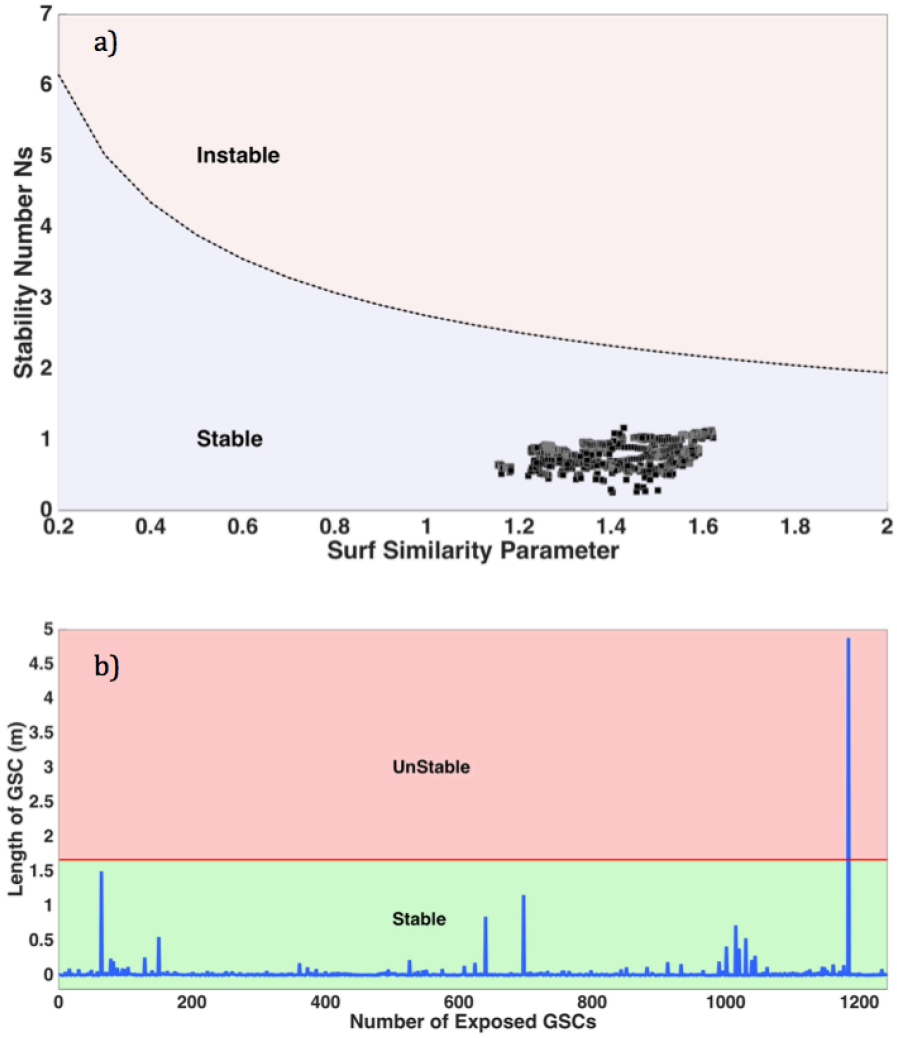


***Figure 2.15*** *Hydraulic Stability analysis for exposed GSCs during TS Hermine using a) Hudson's Based stability equation proposed by Omeraci 2003 and b) Hydraulic Stability proposed by Recio and Omeraci 2007.*

## 6. Discussion

The results of this study allowed us to investigate the adequacy of a selected hydro-morphodynamic model in combination with two GSC hydraulic stability formulas to determine the damage level associated with a reinforced dune with GSC during a storm regime. Damage states associated with the structure were defined and calculated. Further elaboration and discussion of the results is provided in this section.

*6.1 Performance of Hydro-morphodynamic Model*

The ability of XBeach to model the morphological changes of beaches, barrier islands, and dunes have been well validated for collision regime through laboratory and field experiments (Roelvink 2009, 2010; Schambach et al., 2018, Nederhoff, 2014; De Vet et al., 2015; Elsayed and Omeraci, 2017). Good performance was achieved particularly for the region of interest where the GSCs were exposed (Zone B), where accurate morphological predictions were obtained. The simulated eroded volume in Zone A and C is however overestimated by the model, and the longshore sediment transport and deposition on the west was not predicted.

This inaccuracy is expected since XBeach's "Surfbeat" mode has a phase averaged wave module and hence instantaneous velocities are not resolved. Let's also note that the temporal variability of the bathy-topo induces a large uncertainty in the model initial conditions, which can lead to significant variations in the extend of the swash zone, and consequently in the morphological changes of the beach.

*6.2 Performance of Hydraulic Stability Equations*

Hudson's based stability equations seem to underestimate the critical stability of the GSC. Several locations became vulnerable during TS Hermine, which was not detected by Hudson's based stability equations. These equations estimate the stability as a function of the significant wave height at the toe of the structure. Throughout the storm regime, the water depth at that location remained very shallow, and thus most short waves have been saturated. The dominant velocities are therefore generated by the uprush and downrush of the infragravity waves (e.g. Devet et al., 2015; Longuet-Higgins and Stewart, 1964).

The semi-empirical stability formulas such as introduced by Recio and Omeraci (2008) however suggested possible instabilities during TS Hermine, which was verified during the post storm surveys. Although the applicability of these equations to this study remains questionable, since Recio and Omeraci (2008) hydraulic stability equations have been validated for structures with 45 degrees slope (i.e. 1:1). The structure at the project site was constructed with a slope of 1:2, thus giving less contact area around the perimeter of the GSC. Different force coefficients calibration might be required for a 1:2 slope since this increases the effective area and hence the resultant forces and moments.

## 7. Conclusion

Assessment tools are required to determine the fragility of a reinforced dune system with GSC during a storm regime. This study presented a numerical model that identifies the damage states associated with these structures. The model combines an existing hydro-morphodynamic software package "XBeach", with two available hydraulic stability equations for GSC. A Hudson's (1956) based stability equation proposed by Oumeraci (2003) was compared with a more semi-empirical equation proposed by Recio and Oumeraci (2008).

XBeach model was used to determine the initial damage states of erosion, while the hydraulic stability equations were used determine the stability of exposed GSCs. The model was validated against post storm measurements taken after TS Hermine, which caused exposure and minor damage to the GSC at the USACE project site. Results of bed level changes and eroded volume showed excellent performance in the region of interest, while some discrepancies occurred in other regions. Appropriate damage states as occurred during the storm was identified by the model, and consisted mainly of berm and

cover layer erosion up to exposure of the GSC layer. The study indicated better confidence was obtained when using Recio and Omeraci (2008) stability equation for the exposed GSC, however the validity of this equation to the configuration of the structure used in this study remains questionable.

**Acknowledgements**

This research was supported by a grant from the National Science Foundation (CMMI #1719671). The support of the State of Rhode Island Coastal Resources Management Council, Lynn Bocamazo, P.E., D.CE and her staff (U.S. Army Engineer District, New York), Kimberly Shaw and her staff (Town of East Hampton), Aram Terchunian and Benjamin Spratford (First Coastal Corporation), is acknowledged and greatly appreciated.

**References**

Antón, A.I., De la Peña, J.M., Almazán, J.L. and Lechuga, A., 2016. Appropriate Locations for Geotextile Bag Revetments: An Analysis. *Journal of Coastal Research*, *32*(6), pp.1456-1463.

Baquerizo, A. and Losada, M.A., 2008. Human interaction with large scale coastal morphological evolution. An assessment of the uncertainty. *Coastal Engineering*, *55*(7-8), pp.569-580.

Blake, E.S., Kimberlain, T.B., Berg, R.J., Cangialosi, J.P. and Beven Ii, J.L., 2013. Tropical cyclone report: Hurricane sandy. *National Hurricane Center*, *12*, pp.1-10.

Bouyze, J.G. and Schram, A.R., 1990. Stabiliteit van Grondkribben en Onderwatergolbreakers Opgebouwd uit Zandworsten, *TU-Delft, Studentarbeit*.

Coghlan, I., Carley, J., Cox, R., Blacka, M., Mariani, A., Restall, S., Hornsey, W. and Sheldrick, S., 2009. Two-dimensional physical modelling of sand filled Geocontainers for coastal protection. *Coasts and Ports 2009: In a Dynamic Environment*, p.295.

Dassanayake, D.T. and Oumeraci, H.O.C.I.N.E., 2012. Engineering properties of geotextile sand containers and their effect on hydraulic stability and damage development of low-crested/submerged structures. *The International Journal of Ocean and Climate Systems*, *3*(3), pp.135-150.

Dassanayake, D.T. and Oumeraci, H., 2013. Hydraulic stability formulae and nomograms for coastal structures made of geotextile sand containers. In *Proceedings of the 7th International Conference on Asian and Pacific Coasts* (pp. 24-26).

De Vet, P.L.M., McCall, R.T., Den Bieman, J.P., Stive, M.J. and Van Ormondt, M.A.A.R.T.E.N., 2015. Modelling dune erosion, overwash and breaching at Fire Island (NY) during Hurricane Sandy. In *The Proceedings of the Coastal Sediments 2015*.

Elsayed, S.M. and Oumeraci, H., 2017. Effect of beach slope and grain-stabilization on coastal sediment transport: An attempt to overcome the erosion overestimation by XBeach. *Coastal Engineering*, *121*, pp.179-196.

Gallagher, E.L., Elgar, S. and Guza, R.T., 1998. Observations of sand bar evolution on a natural beach. *Journal of Geophysical Research: Oceans*, *103*(C2), pp.3203-3215.

Galappatti, G. and Vreugdenhil, C.B., 1985. A depth-integrated model for suspended sediment transport. *Journal of Hydraulic Research*, *23*(4), pp.359-377.

Grilli, A.R., Grilli, S.T., David, E. and Coulet, C., 2015, July. Modeling of Tsunami Propagation in the Atlantic Ocean Basin for Tsunami Hazard Assessment along the North Shore of Hispaniola. In *The Twenty-fifth International Ocean and Polar Engineering Conference*. International Society of Offshore and Polar Engineers.

Grilli, A.R., Spauding, M.L., Schambach, L., Smith, J. and Bryant, M., 2017a. Comparing Inundation Maps Developed Using WHAFIS and STWAVE: A Case Study in Washington County, RI. *Proceeding of the ASCE conference: Coastal Structures and Solutions to Coastal Disasters 2015 : Resilient Coastal Communities* **.**

Grilli, A., Spaulding, M.L., Oakley, B.A. and Damon, C., 2017b. Mapping the coastal risk for the next century, including sea level rise and changes in the coastline: application to Charlestown RI, USA. *Natural Hazards*, *88*(1), pp.389-414.

Grilli, S.T., Guérin, C.A., Shelby, M., Grilli, A.R., Moran, P., Grosdidier, S. and Insua, T.L., 2017c. Tsunami Detection by High Frequency Radar Beyond the Continental Shelf: II. Extension of Time Correlation Algorithm and Validation on Realistic Case Studies. *Pure and Applied Geophysics*, *174*(8), pp.3003-3028.

Hornsey, W.P., Carley, J.T., Coghlan, I.R. and Cox, R.J., 2011. Geotextile sand container shoreline protection systems: Design and application. *Geotextiles and Geomembranes*, *29*(4), pp.425-439.

Hudson, R.Y., 1959. Laboratory investigation of rubble-mound breakwaters. *Reprint of the original paper as published in the Journal of the Waterways and Harbors Division of ASCE, proceedings paper 2171*.

Jacobs, B.K. and Kobayashi, N., 1983. *Sandbag Stability and Wave Runup on Bench Slopes*. Ocean Engineering Program, Department of Civil Engineering, University of Delaware.

Longuet-Higgins, M.S. and Stewart, R.W., 1964, August. Radiation stresses in water waves; a physical discussion, with applications. In *Deep Sea Research and Oceanographic Abstracts* (Vol. 11, No. 4, pp. 529-562). Elsevier.

Mitsuyasu, H., Tasai, F., Suhara, T., Mizuno, S., Ohkusu, M., Honda, T. and Rikiishi, K., 1975. Observations of the directional spectrum of ocean WavesUsing a cloverleaf buoy. *Journal of Physical Oceanography*, *5*(4), pp.750-760.

Mori, E., D'eliso, C. and Aminti, P.L., 2008, July. Physical modelling on geotextile sand container used for submerged breakwater. In *Proceedings of 2nd international conference on the application of physical modelling to port and coastal protection, Coastlab08, Bari, Italy*.

Nederhoff, K., 2014. Modeling the effects of hard structures on dune erosion and overwash; Hindcasting the impact of Hurricane Sandy on New Jersey with XBeach. *Master's thesis Delft University of Technology*.

Oumeraci, H., Hinz, M., Bleck, M. and Kortenhaus, A., 2003. Sand-filled geotextile containers for shore protection. *COPEDEC VI, Colombo, Sri Lanka*.

Pilarczyk, K., 2000. *Geosynthetics and geosystems in hydraulic and coastal engineering*. CRC Press.

Raubenheimer, B., Guza, R.T. and Elgar, S., 1996. Wave transformation across the inner surf zone. *Journal of Geophysical Research: Oceans*, *101*(C11), pp.25589-25597

Recio, J. and Oumeraci, H., 2007. Effect of deformations on the hydraulic stability of coastal structures made of geotextile sand containers. *Geotextiles and geomembranes*, *25*(4-5), pp.278-292.

Recio, J.A. and Oumeraci, H., 2008. *Hydraulic stability of geotextile sand containers for coastal structures* (Doctoral dissertation, PhD-Thesis Univ. of Braunschweig, Germany, Faculty of Architecture, Civil Engineering and Environment).

Recio, J. and Oumeraci, H., 2009. Hydraulic stability of geotextile sand containers for coastal structures–effect of deformations and stability formulae. In *Coastal Engineering 2008: (In 5 Volumes)* (pp. 3805-3817).

Roelvink, D., Reniers, A., Van Dongeren, A.P., de Vries, J.V.T., McCall, R. and Lescinski, J., 2009. Modelling storm impacts on beaches, dunes and barrier islands. *Coastal engineering*, *56*(11-12), pp.1133-1152.

Roelvink, D., Reniers, A.J.H.M., Van Dongeren, A., Van Thiel de Vries, J., Lescinski, J. and McCall, R., 2010. XBeach model description and manual. *Unesco-IHE Institute for Water Education, Deltares and Delft University of Tecnhology. Report June*, *21*, p.2010

Roelvink, D., McCall, R., Mehvar, S., Nederhoff, K. and Dastgheib, A., 2018. Improving predictions of swash dynamics in XBeach: The role of groupiness and incident-band runup. *Coastal Engineering*, *134*, pp.103-123

Sallenger Jr, A.H., 2000. Storm impact scale for barrier islands. *Journal of Coastal Research*, pp.890-895.

Schambach, L., Grilli, A.R., Grilli, S.T., Hashemi, M.R. and King, J.W., 2018. Assessing the impact of extreme storms on barrier beaches along the Atlantic coastline: Application to the southern Rhode Island coast. *Coastal Engineering*, *133*, pp.26-42.

Shirlal, K.G. and Mallidi, R.R., 2015. Physical model studies on stability of geotextile sand containers. *Procedia Engineering*, *116*, pp.567-574.

Small, C., Blanpied, T., Kauffman, A., O'Neil, C., Proulx, N., Rajacich, M., Simpson, H., White, J., Spaulding, M.L., Baxter, C.D. and Swanson, J.C., 2016. Assessment of Damage and Adaptation Strategies for Structures and Infrastructure from Storm Surge and Sea Level Rise for a Coastal Community in Rhode Island, United States. *Journal of Marine Science and Engineering*, *4*(4), p.67.

Smith, J.M., Sherlock, A.R. and Resio, D.T., 2001. *STWAVE: Steady-state spectral wave model user's manual for STWAVE, Version 3.0* (No. ERDC/CHL-SR-01-1). Engineer Research and Development Center Vickburg MS Coastal and Hydraulics Lab.

Soulsby, R.L. and Whitehouse, R.J.S., 1997. Threshold of sediment motion in coastal environments. In *Pacific Coasts and Ports' 97: Proceedings of the 13th Australasian Coastal and Ocean Engineering Conference and the 6th Australasian Port and Harbour Conference; Volume 1* (p. 145). Centre for Advanced Engineering, University of Canterbury.

Spaulding, M.L., Grilli, A., Damon, C., Crean, T., Fugate, G., Oakley, B.A. and Stempel, P., 2016. STORMTOOLS: coastal environmental risk index (CERI). *Journal of Marine Science and Engineering*, *4*(3), p.54.

Spaulding, M.L., Grilli, A., Damon, C., Fugate, G., Isaji, T. and Schambach, L., 2017. Application of State of the Art Modeling Techniques to Predict Flooding and Waves for a Coastal Area within a Protected Bay. *Journal of Marine Science and Engineering*, *5*(1), p.14.

Svendsen, I.A., 1984. Mass flux and undertow in a surf zone. *Coastal Engineering*, *8*(4), pp.347-365.

Tekmarine Inc, 1982. Larg-scale model studies of arctic island slope protection. Sierra California.

USACE-NAN, 2014. *Downtown Montauk Stabilization Project: Hurricane Sandy Limited Reevaluation Report*. U.S. Army Corps of Engineers, New York District.

Van Rijn, L.C., 1989. The state of the art in sediment transport modelling. In *Sediment Transport Modeling* (pp. 13-32). ASCE.

Van Rijn, L.C., Walstra, D.J.R., Grasmeijer, B., Sutherland, J., Pan, S. and Sierra, J.P., 2003. The predictability of cross-shore bed evolution of sandy beaches at the time scale of storms and seasons using process-based profile models. *Coastal Engineering*, *47*(3), pp.295-327.

Van Rijn, L.C., 2007. Unified view of sediment transport by currents and waves. I: Initiation of motion, bed roughness, and bed-load transport. *Journal of hydraulic engineering*, *133*(6), pp.649-667.

Van Rooijen, A.A., 2011. Modelling sediment transport in the swash zone.

Van Thiel de Vries, J.S.M., 2009. Dune erosion during storm surges

Vitousek, S., Barnard, P.L., Fletcher, C.H., Frazer, N., Erikson, L. and Storlazzi, C.D., 2017. Doubling of coastal flooding frequency within decades due to sea-level rise. *Scientific reports*, *7*(1), p.1399.

Woodruff, J.D., Irish, J.L. and Camargo, S.J., 2013. Coastal flooding by tropical cyclones and sea-level rise. *Nature*, *504*(7478), p.44.

Wouters, J., 1998. Open Taludbekledingen; stabiliteit van geosystems (Stability of Geosystems). *Delft Hydraulics*, (H1939).